

1 Studying attention to IPCC climate change maps with mobile eye-
2 tracking

3 Doga Gulhan^{*,1,2}, Bahador Bahrami², Ophelia Deroy³

4 ¹Department of Psychology, Royal Holloway, University of London, UK

5 ²Faculty of General Psychology and Education, Ludwig Maximilian University of Munich, Germany

6 ³Faculty of Philosophy, Philosophy of Science and the Study of Religion, Ludwig Maximilian University of Munich,
7 Germany

8 *Corresponding author contact information: dogagulhan@gmail.com (DG)

9 **I. Abstract**

10 Many visualisations used in the climate communication field aim to present the scientific
11 models of climate change to the public. However, relatively little research has been conducted
12 on how such data are visually processed, particularly from a behavioural science perspective.
13 This study examines trends in visual attention to climate change predictions in world maps
14 using mobile eye-tracking while participants engage with the visualisations. Our primary aim is
15 to assess engagement with the maps, as indicated by gaze metrics. Secondary analyses assess
16 whether social context (as social viewing compared to solitary viewing) affects these trends, the
17 relationship between projection types and visual attention, compare gaze metrics between
18 scientific map and artwork viewing, and explore correlations between self-reported climate
19 anxiety scores and attention patterns. We employed wearable, head-mounted eye-tracking to
20 collect data in relatively naturalistic conditions, aiming to enhance ecological validity. In this
21 research, participants engaged with ten world maps displaying near- and far-term climate
22 projections across five data categories, adapted from the online interactive atlas provided by the
23 International Panel on Climate Change (IPCC). To compare scientific information processing
24 with aesthetic perception, participants also viewed two large-scale artworks. Responses to the
25 Climate Change Anxiety Scale (CCAS) were also collected. Participants viewed the displays
26 alone (single-viewing condition, N=35) or together with a partner (paired-viewing condition,
27 N=12). Results revealed that the upper parts of the maps, particularly the continental Europe,
28 received significant attention, suggesting a Euro-centric bias in viewing patterns. Spatial gaze
29 patterns were similar between single and paired conditions, indicating that the visual attributes
30 of the maps predominantly shaped attention locations. Although dwell times were comparable,
31 the paired condition showed higher fixation counts, shorter average fixation durations, and
32 longer scanpaths, suggesting a potentially dissociable viewing strategy and more exploratory
33 viewing patterns influenced by social interaction. No substantial differences were observed in

34 attention across projection timeframes or types, although individual variations were noted.
35 Artwork viewing exhibited notably shorter average fixation durations compared to climate map
36 viewing, potentially reflecting different visual engagement styles. Despite positive linear
37 correlations among the four CCAS subscales, there was no apparent correlation between CCAS
38 scores and main gaze metrics, indicating a lack of a direct relationship between self-reported
39 anxiety and gaze behaviour. In summary, visual attention to climate change visualisations
40 appears to be mainly influenced by the inherent visual attributes of the maps, but the social
41 context may subtly influence visual attention. Additionally, the comparison with aesthetic
42 viewing highlights relatively distinct attentional patterns in scientific versus aesthetic
43 engagements.

44 **Keywords:** Climate communication, IPCC maps, mobile eye-tracking, visual
45 attention, social viewing, aesthetic perception

46 2. Introduction

47 Most of us have seen maps of the earth, often coloured in shades of red and dark orange,
48 illustrating the predicted rise in temperature or rainfalls over the coming decades. But beyond
49 the broad message that we probably already knew, what did we pay attention to? Maps are a
50 major instrument for reporting and communicating climate change to journalists, politicians,
51 and the wider public [1]. They can convey a rich wealth of the spatial, temporal, and
52 quantitative information agreed upon by the community in a simpler and more vivid manner
53 [2]. Maps make up more than 25% of the visualisations in the annual reports of the
54 International Panel on Climate Change (IPCC). These often global representations are widely
55 circulated and used for further decisions and communication campaigns. The IPCC has
56 invested efforts into building better maps and visualisations [3], although suggestions from
57 researchers for more solution-oriented framing [4] remain valid criticism. Nevertheless,

58 intuitions of experts on what constitutes good design in data visualisation do not always
59 materialise, making it important to test data visualisations with the public empirically.

60 While map-viewing in general is being explored in various contexts through eye-
61 tracking, aiming to answer a wide range of research questions [5–12], we know little about how
62 people specifically look at world maps, particularly those visualising climate change. This gap
63 can be surprising given how much the behavioural sciences have contributed to climate science
64 communication by measuring public perceptions and attitudes toward the crisis, and how many
65 recommendations for improving visualisations they have made over the years [1,13,14], along
66 with improving textual contents [15]. While a few studies have recently confirmed the
67 effectiveness of climate communication with maps [16], other studies raise concerns about
68 possible biases induced by the same visualisations, for instance through the misuse of colour
69 [17,18]. In parallel, research on artwork perception highlights the importance of viewing
70 context (such as laboratory versus gallery or museum environments, spatial layouts, and the
71 authenticity of artworks) in shaping engagement and judgment, with distinct patterns emerging
72 between categories such as digital versus physical or genuine versus replica [19–26]. However,
73 comparisons between aesthetic and scientific viewing contexts remain underexplored, offering
74 a promising direction for further investigation.

75 To assess public responses and provide evidence-based recommendations, it is essential
76 to move to flexible and varied data collection methodologies beyond traditional questionnaires
77 and focus groups. To address this, we demonstrate the feasibility and relevance of collecting
78 behavioural data from the public as they engage with climate communications and, briefly, with
79 reproduction of artworks, *in situ*. Mobile eye-tracking technology provides a relatively objective
80 and unobtrusive means to measure where viewers direct their attention when engaging with
81 visual stimuli. It is adaptable for use on screens, mobile devices, and in virtual reality, and can
82 be scaled up to widespread, *in situ* implementation.

83 Our study primarily aimed to deploy and validate mobile eye-tracking in a controlled
84 lab setting to investigate how individuals direct their visual attention to climate projection maps.
85 Secondarily, the study also explored potential differences in visual engagement with scientific
86 versus aesthetic stimuli, providing preliminary insights into how people process information-
87 oriented maps compared to visually expressive artworks, while recognising that engagement in
88 lab-based engagement may differ from that in museum environments. While eye-tracking
89 captures gaze in an agnostic way, it is often assumed that distinct pre-attentive (commonly
90 associated with bottom-up processes) and attentive (commonly associated with top-down
91 processes) mechanisms exist. Arguably, our research primarily focuses on bottom-up responses,
92 where participants' gaze is likely driven by factors such as the visual saliency of the maps,
93 reflecting early, pre-attentive processing, but also influenced by top-down factors like prior
94 knowledge on the issue. To approximate the viewing conditions that the public may encounter
95 in museums or classrooms, we compared solitary viewing conditions to social conditions, where
96 two individuals looked at the same item at the same time. Here, we tested climate change maps
97 as projected data from the IPCC, and included two artworks, to examine differences between
98 viewing patterns aimed at gathering information versus aesthetic appreciation. We aimed to
99 evaluate the utility of mobile eye-tracking as a tool for collecting data on a large scale outside of
100 lab settings, such as during exhibitions, public events, and in educational settings. Ultimately,
101 understanding public behavioural responses, such as visual attention to climate change
102 visualisations, can yield insights that enhance design strategies, making visualisations more
103 explanatory and inclusive.

104 **3. Methods**

105 **3.1. Participants**

106 This study initially recruited 50 participants through convenience sampling. Three
107 recordings were excluded because the gaze mapping algorithm failed to normalise fixation data,
108 and three additional participants did not provide questionnaire responses. The final sample
109 included 47 participants for gaze analysis and 44 for questionnaire responses (33 females, 8
110 males, 1 non-binary, 2 unspecified; $M_{Age} = 20.93$ years, $SD_{Age} = 4.14$ years, $R_{Age} = 18\text{--}37$
111 years). Participants, primarily students and staff from Royal Holloway, University of London,
112 were recruited via online platforms and campus flyers.

113 All participants provided written informed consent. The research protocols were
114 certified by the researcher in accordance with the self-certification guidelines provided by the
115 Research Ethics Committee at Royal Holloway, University of London (approval ID: 3527-
116 TFJT002, 2022-12-02). The study was conducted in compliance with the ethical standards
117 outlined in the Declaration of Helsinki. The recruitment period spanned from 05/12/2022 to
118 05/03/2023.

119 Corrective lens inserts were provided for participants requiring glasses where possible,
120 but data from those with high prescriptions or other unusable recordings were excluded.
121 Participants were assigned to either single-viewing ($N = 35$) or paired-viewing conditions ($N =$
122 12, six pairs). Unequal group sizes reflected the practical challenges of recruiting pairs, resulting
123 in more participants in the single-viewing condition. Participants received £5 or course credit
124 as compensation.

125 **3.2. Stimuli and materials**

126 This study utilised two sets of stimuli (maps and artworks), divided into two sequentially
127 conducted parts. The experiment was conducted in the available space of the Virtual Reality
128 (VR) Lab at the Department of Psychology, Royal Holloway, University of London (although
129 participants did not use VR). The primary stimuli for Part 1 consisted of ten world maps

130 displayed on a 17-inch laptop monitor (Dell Alienware 2019), depicting global climate change
131 projections, including near and far future scenarios for five key measures: mean temperature,
132 sea surface temperature, sea level rise, anthropogenic CO₂ emissions, and atmospheric
133 particulate matter concentrations (PM_{2.5}). These maps were generated using data visualisation
134 tools [27,28], provided by the Intergovernmental Panel on Climate Change (IPCC) and were
135 accessible at interactive-atlas.ipcc.ch at the time of writing (see **S1 Fig** for an overview). The
136 supplementary stimuli for Part 2 included two large-scale artworks printed on A0-sized posters
137 and mounted on the laboratory wall (see **S2 Fig** for details).

138 The Climate Change Anxiety Scale (CCAS), a 22-item questionnaire [29], was used to
139 measure participants' responses to climate change on a 5-point Likert scale, covering four
140 subcategories (see **S1 File** for the full scale). An exit-questionnaire was also administered to
141 gather optional demographics data and participant feedback.

142 Gaze data were recorded with the Pupil Invisible mobile eye-tracker using Pupil
143 Invisible Companion App (version 1.4.21). The raw gaze data were pre-processed on the
144 GDPR-compliant Pupil Cloud platform. The maps were presented using PsychoPy (version
145 2022.2.5), the CCAS and exit-questionnaire were presented using Google Forms (see **S3 Fig**
146 for the experimental setup).

147 **3.3. Design**

148 This study was primarily exploratory and descriptive, aiming to analyse participants'
149 viewing patterns using mobile eye-tracking data while they engaged with ten world maps
150 depicting the climate crisis and two artworks in a laboratory setting.

151 Data were collected under two viewing conditions: a primary individual viewing
152 condition, where participants viewed the stimuli alone, and a secondary paired viewing
153 condition, where pairs of participants viewed the stimuli together. Despite challenges in

154 recruiting pairs, which resulted in unequal group sizes (35 and 12 in single- and paired-viewing
155 conditions) the setup allowed for the collection and comparative analysis of gaze metrics across
156 different viewing contexts.

157 The primary analyses focused on fixation-based metrics and their derivatives, which are
158 often linked to attentional processes, such as overt attention and visual attention guidance.
159 Descriptive statistics such as averages, frequencies, and heatmap visualisations were used to
160 present data rather than formal hypothesis testing, highlighting engagement patterns with the
161 stimuli.

162 Additionally, the study served as a preliminary evaluation of the feasibility of the
163 research procedures and the analysis pipeline in a laboratory setting and beyond, establishing
164 groundwork for future in-situ experiments in public spaces. A significant goal was to compile a
165 sizeable eye-tracking dataset, which, due to the inherent limitations of mobile eye-tracking
166 systems, was expected to be noisier than data from stationary systems. Lastly, this open dataset
167 and code were prepared for reuse in future research, allowing for expanded analyses.

168 **3.4. Procedure**

169 The experiment was conducted during regular working hours. Participants began by
170 receiving detailed written and oral instructions, and the experimenter addressed any questions.
171 They provided written informed consent before being equipped with the mobile eye tracker,
172 with correction lens inserts provided when needed. Although the mobile eye tracker was
173 calibration-free and self-correcting, calibration was visually checked using a standard five-point
174 calibration panel, and offset corrections were applied if necessary.

175 For the first part of the experiment (map viewing), participants' calibration was
176 confirmed before the recording started. Each participant was assigned a randomly generated
177 three-digit ID and viewed maps displayed on a laptop in a semi-randomised order, spending at

178 least 30 seconds per map. The near-term projection map of each type was always displayed
179 before the corresponding long-term projection map, but the order of projection types was
180 randomised across participants (see **S4 Fig** for the procedure diagram). Participants in the
181 paired-viewing condition were encouraged to discuss the maps with their partner, while those
182 in the single-viewing condition viewed them independently.

183 For the second part (artwork viewing), participants viewed two large-scale paintings
184 mounted on the wall. They carried the companion device with them and were free to choose
185 the viewing order and spend as much time as they wished on the artworks, moving freely around
186 them.

187 After both sessions, participants filled out the 22-item climate change anxiety scale and
188 optionally provided demographic information and comments. The experiment concluded with
189 a debriefing by the experimenter.

190 **3.5. Data analysis**

191 Data analysis progressed through several stages, from raw recordings to detailed
192 analyses. Recordings from the companion device were uploaded to Pupil Cloud, a GDPR-
193 compliant online platform for data processing and visualisation. Fixation detection used an
194 extended I-VT (Identification by Velocity Threshold) algorithm. Data quality was inspected
195 informally by visually checking raw gaze data overlaid with fixations on Pupil Cloud, alongside
196 fixation duration rates relative to recording duration. No valid recordings were excluded. Some
197 spatiotemporal random noise in gaze data, as reported by the manufacturer, was assumed not
198 to affect the primarily descriptive analyses.

199 To map the XY-coordinates of raw gaze and fixation data, two streams of parallel
200 processing were employed on the cloud. This dual approach was designed to take advantage of
201 a newly available algorithm in beta version at the time of data collection, which was later

202 released as a stable version. The first, marker mapper enrichment (MME), utilised fiducial
203 markers (Apriltags) placed around the laptop monitor and paintings to define areas of interest
204 (AOIs). Recordings were manually time-stamped for segmentation, and markers served as
205 anchor points to normalise gaze data. The second, reference image mapper (RIM), employed
206 video recordings and snapshots to create a structure-from-motion model for normalisation.
207 While both methods produced comparable data structures, RIM demonstrated higher accuracy
208 and was used for all subsequent analyses (see **S5 Fig** for an overview). RIM preserved the
209 height-to-width ratio of stimuli in pixel-based values, unlike MME, which distorted the aspect
210 ratio during normalisation. Surface-normalised fixation data were used to create heatmaps
211 visualising viewing patterns.

212 The enriched dataset, along with supplementary materials, was uploaded to Kaggle and
213 Google Colab for further analysis using Python-based notebooks (e.g., pandas, matplotlib,
214 seaborn), alongside offline software (e.g., jamovi). Affinity Designer and Affinity Photo were
215 used to refine plot outputs. Data and analyses were also uploaded to the Open Science
216 Framework (osf.io). Primary gaze metrics included total fixation duration (in milliseconds and
217 percentage), fixation count, average fixation duration, and proxy saccadic scanpath length. As
218 mobile eye tracking lacked constant participant-to-stimulus distance, scanpath length was
219 calculated using pixel-based on-screen values as a proxy.

220 **4. Results**

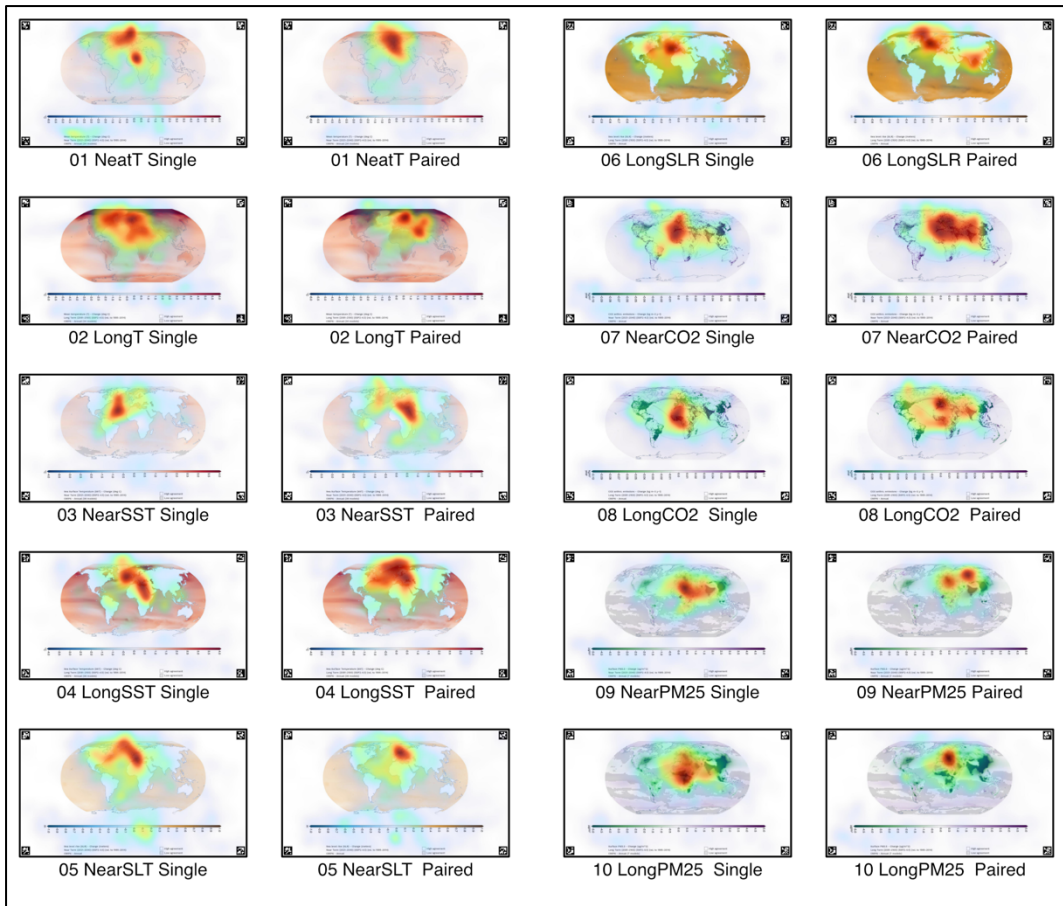
221 The results section generally reports descriptive values, specifically the mean (M) and
222 standard error of the mean ($\pm SEM$), unless stated otherwise. The primary indicators of
223 participant engagement with the maps and artworks were derived from fixation-based metrics,
224 including total fixation duration (also referred to as dwell time), fixation count, average fixation
225 duration, and proxy saccadic scanpath length. Instances of transient engagement, such as brief

226 glances at fiducial markers, were excluded from the analysis due to their minimal duration. As
227 previously described in the Data Analysis section, the pre-processed, enriched data were
228 obtained using the reference image mapper (RIM) technique.

229 **4.1. Descriptive statistics for maps**

230 The main descriptive statistics for the maps reflect averages across all stimuli, without
231 differentiation by map type. Supplementary statistics were broken down either by map
232 projection timeframe or projection type. Sample sizes were 35 for the single viewing condition
233 and 12 for the paired viewing condition, with each of the 10 stimuli viewed under both
234 conditions. This resulted in a total of 350 observations for the single viewing and 120 for the
235 paired viewing conditions.

236 Initial visualisation using cumulative heatmaps revealed a strong upper-central tendency
237 in viewing patterns, indicating that regions on and around continental Europe received
238 significant attention across most cases. These heatmaps also illustrated comparable spatial
239 patterns between single and paired viewing conditions. Notably, a considerable number of
240 fixations were concentrated on the scales and on areas of the maps displaying the minima and
241 maxima values of the corresponding scale. These areas often represent the most salient regions
242 in terms of contrast and colour, suggesting that such bottom-up factors are major determinants
243 of spatial attention location among participants. For an illustrative overview of these patterns,
244 refer to **Fig 1**, which displays the heatmaps of the maps.



245 **Fig 1. Fixation heatmaps for maps.** Heatmaps illustrate fixation distributions across maps
 246 under single and paired-viewing conditions, using a green-to-red colour scale for shorter to longer
 247 fixation durations. Single- and paired-viewing conditions are shown in the first/third and
 248 second/fourth columns, respectively. Spatial common ground generally exhibits an upper-central
 249 tendency. Substantial overlap between conditions suggests that image-based saliency predominantly
 250 drives visual attention, over social context.

251 In comparing single and paired viewing conditions ($N_{\text{SampleSingle}} = 35$, $N_{\text{StimulusSingle}} = 350$
 252 and ($N_{\text{SamplePaired}} = 12$, $N_{\text{StimulusPaired}} = 120$), the total fixation duration, or dwell time, averaged
 253 around 30 seconds per map, showing some variations within each condition but relatively
 254 minimal variation between conditions: $M_{\text{Single}} = 29.70 \text{ s } (\pm .25)$, $M_{\text{Paired}} = 32.92 \text{ s } (\pm .94)$. This
 255 represented approximately 10% of the total dwell time across each map for both conditions.
 256 The number of fixations, or fixation count, was relatively lower in the single viewing condition
 257 compared to the paired viewing condition: $M_{\text{Single}} = 55.12 \text{ } (\pm .87)$, $M_{\text{Paired}} = 70.70 \text{ } (\pm 2.47)$. In

line with this difference in the fixation count, and as a derivative metric to the previous two, the average fixation duration was longer in the single viewing condition compared to the paired viewing condition: $M_{\text{Single}} = 586.43 \text{ ms} (\pm 11.29)$, $M_{\text{Paired}} = 504.45 \text{ ms} (\pm 15.29)$. The proxy scanpath length, measured as the cumulative sum of Euclidean distances between successive fixations based on reference images with 1920×1080 pixel dimensions, was shorter in the single viewing condition compared to the paired viewing condition: $M_{\text{Single}} = 19534.89 \text{ px} (\pm 365.87)$, $M_{\text{Paired}} = 26288.61 \text{ px} \pm 1036.95$), refer to **Fig 2** for an overview as barplots and **S1 Table** for aggregate metrics.

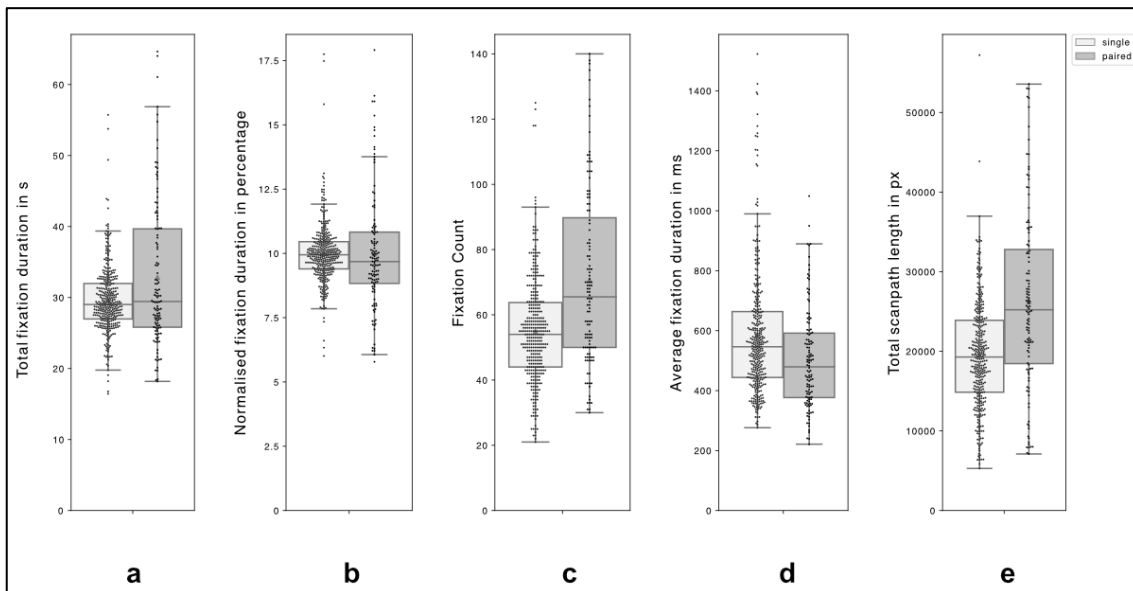


Fig 2. Box plots of gaze metrics for maps. Box plots illustrate five gaze metrics across all maps (single-viewing in light grey and paired-viewing in dark grey): **(a)** total fixation duration (s), **(b)** normalised fixation duration (%), **(c)** fixation count, **(d)** average fixation duration (ms), and **(e)** proxy scanpath length (pixels). Whilst total fixation durations were comparable between conditions, paired viewing showed higher fixation counts, shorter average fixation durations, and longer scanpaths. Each plot displays the range (excluding outliers), interquartile range, median, and mean (triangle overlay).

Despite the relatively low sample size and exploratory nature of the research, a nonparametric ANOVA (Kruskal-Wallis test) was used to analyse these metrics. While fixation duration showed no significant differences, fixation count, average fixation duration, and

276 scanpath length displayed significant differences between single and paired viewing conditions
277 (see **S2 Table** for detailed breakdown of χ^2 , df, p, ϵ^2 values)

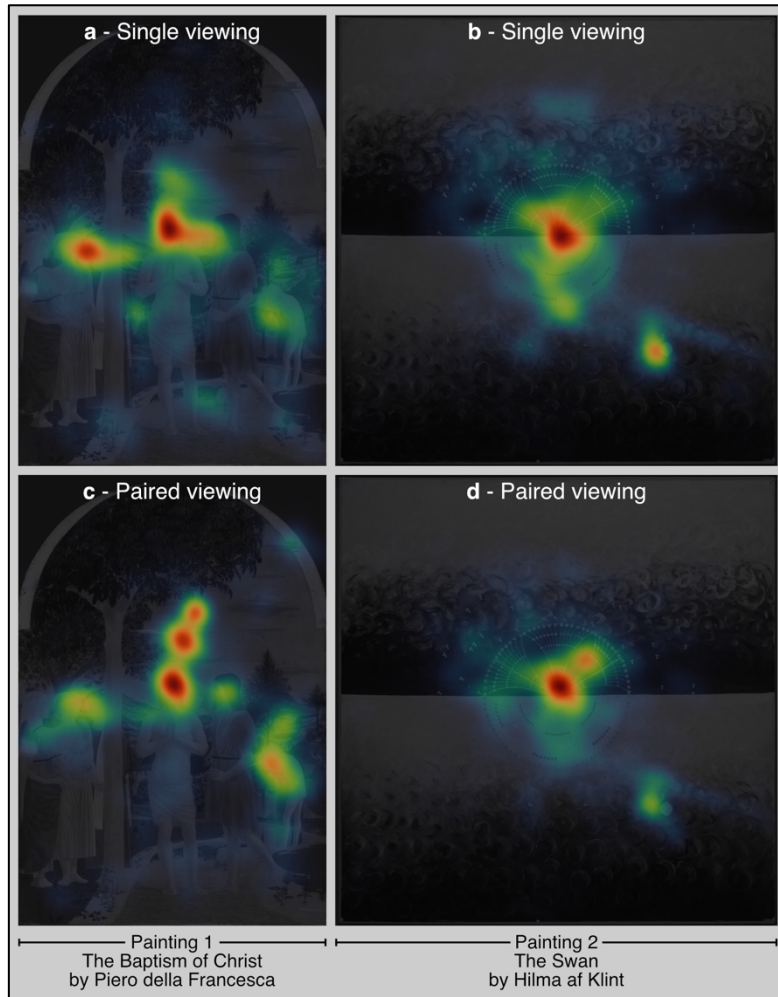
278 Additionally, descriptive statistics were reported based on two categorisations: map
279 projection timeframe (near and far future) and map projection type (main temperature, sea
280 surface temperature, sea level rise, anthropogenic CO₂ emissions, and fine particulate matter
281 PM_{2.5}). Metrics were similar between the two timeframes but showed some variation across the
282 five types of projections. The overall variance was generally larger, especially for the maximas,
283 in paired condition for all metrics except average fixation duration. These results are presented
284 in **S3 Table**. To further illustrate minor trends and detailed data across the five metrics, results
285 were divided by both viewing conditions and the ten stimuli. **S6 Fig** displays bar plots overlaid
286 with individual data points, and **S4 Table** provides a comprehensive descriptive summary.

287 Lastly, given the inherent gaze-estimation accuracy limits of the mobile eye tracker
288 (approximately reported as $\approx 4^\circ$ by the whitepaper from the manufacturer), conducting a highly
289 granular AOI-based analysis may lead to significant errors: particularly for a generic viewing
290 condition, the monitor surface area might roughly translate to a surface of a $38^\circ \times 21.5^\circ$ of
291 visual angles. For instance, it is impractical to confidently display fixations on individual
292 countries due to these accuracy limitations and the relatively low sample size, which could skew
293 the gaze estimation errors beyond mere random noise in the data. Nevertheless, as a proof of
294 concept, the stimulus was divided into two broad AOIs: the upper section representing the map
295 and the lower section the scale. On average, participants spent four times as much time viewing
296 the main map compared to the scale at the bottom. This 80-20% relative dwell time difference
297 was interestingly consistent across both viewing conditions and remained relatively stable when
298 broken down by individual maps (see **S5 Table**).

299 **4.2. Descriptive statistics for paintings**

300 Similar to the analysis of the maps, descriptive statistics for the two paintings were
301 calculated, averaging across stimuli. Sample sizes were 35 for the single viewing condition and
302 12 for the paired viewing condition, with each of the two stimuli viewed under both conditions.
303 This resulted in a total of 70 observations for the single viewing and 24 for the paired viewing
304 conditions.

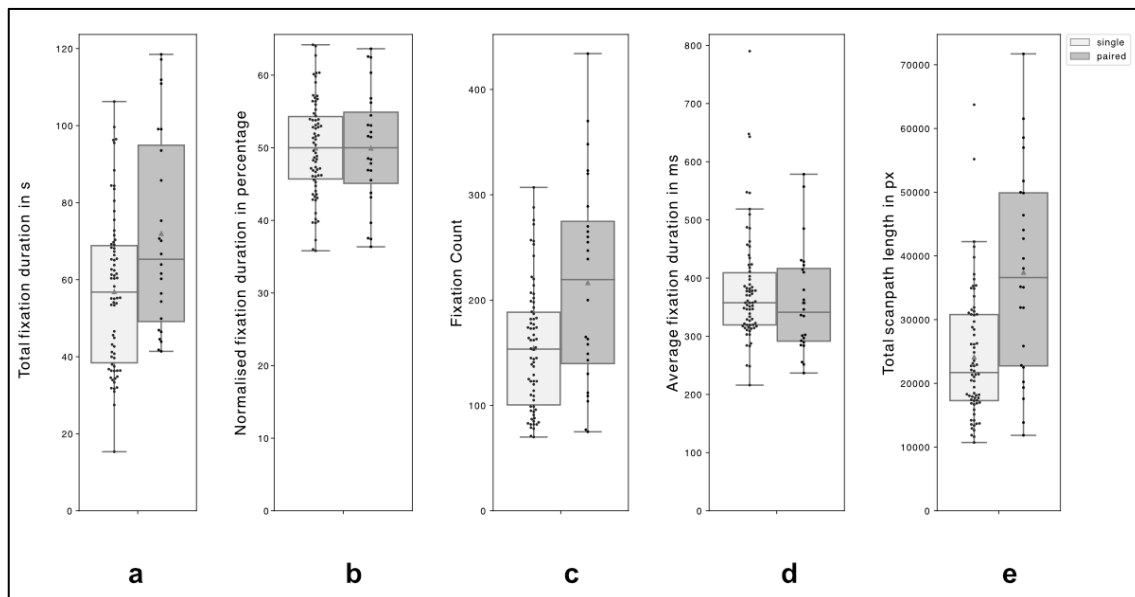
305 Initial visualisation using cumulative heatmaps for the paintings indicated a pronounced
306 central tendency consistent with the layout of the artworks. The first painting, being more
307 figurative with numerous elements, exhibited diverse focal points such as faces and bodies,
308 resulting in a more dispersed gaze pattern across both X and Y axes. In contrast, the second
309 painting, which is more abstract and centrally composed, showed gaze dispersion primarily
310 concentrated at the centre and one particular area on bottom-right (albeit gaze dispersions were
311 not further plotted). These differences highlight how compositional elements influence visual
312 attention as indexed by cumulative fixations. For a detailed view of these attentional
313 distributions, refer to **Fig 3**, showcasing the heatmaps of the paintings.



314 **Fig 3. Fixation heatmaps for paintings.** Heatmaps show fixation distributions for two
 315 paintings, based on data from all participants in both single-viewing (**a-b**) and paired-viewing (**c-**
 316 **d)** conditions.

317 In comparing single and paired viewing conditions ($N_{\text{SampleSingle}} = 35$, $N_{\text{StimulusSingle}} = 75$
 318 and ($N_{\text{SamplePaired}} = 12$, $N_{\text{StimulusPaired}} = 24$), the total fixation duration, or dwell time, averaged
 319 about one minute per painting, with some variation within each condition and slightly shorter
 320 durations in the single condition compared to the paired: $M_{\text{Single}} = 56.97 \text{ s} (\pm 2.40)$, $M_{\text{Paired}} =$
 321 $72.09 \text{ s} (\pm 5.30)$. The number of fixations, or fixation count, was relatively lower in the single
 322 viewing condition compared to the paired: $M_{\text{Single}} = 154.87 (\pm 7.07)$, $M_{\text{Paired}} = 216.86 (\pm 20.27)$.
 323 Additionally, the average fixation duration was only slightly longer in the single viewing
 324 condition: $M_{\text{Single}} = 380.51 \text{ ms} (\pm 11.41)$, $M_{\text{Paired}} = 359.95 \text{ ms} (\pm 18.68)$. The proxy scanpath

325 length, measured as the cumulative sum of Euclidean distances between successive fixations
 326 based on reference images (685×1000 pixels for the Baptism of Christ (Painting #1) and 983
 327 $\times 1000$ pixels for The Swan (Painting #2)), was significantly shorter in the single viewing
 328 condition: $M_{\text{Single}} = 24196.75 \text{ px} (\pm 1205.88)$, $M_{\text{Paired}} = 37468.70 \text{ px} (\pm 3332.50)$, refer to **Fig 4**
 329 for an overview as barplots and **S6 Table** for aggregate metrics, divided by viewing two
 330 conditions.



331 **Fig 4. Box plots of gaze metrics for paintings.** Box plots depicts five gaze metrics for
 332 two paintings (single-viewing in light grey and paired-viewing in dark grey): **(a)** total fixation
 333 duration (s), **(b)** normalised fixation duration (%), **(c)** fixation count, **(d)** average fixation duration
 334 (ms), and **(e)** proxy scanpath length (pixels). On average, single viewing showed slightly shorter
 335 dwell times, lower fixation counts, slightly longer average fixation durations, and significantly
 336 shorter scanpath lengths. Each plot shows the range (excluding outliers), interquartile range,
 337 median, and mean (triangle overlay).

338 Despite the relatively low sample size and the exploratory nature of the research, a
 339 nonparametric ANOVA (Kruskal-Wallis test) was employed for statistical analysis. While
 340 average fixation duration showed no significant differences, total fixation duration, fixation
 341 count, and scanpath length exhibited significant differences across conditions (see **S7 Table** for

342 a detailed breakdown of χ^2 , df, p, ϵ^2 . Similar trends were observed when the data were further
343 disaggregated by the two paintings (see **S7 Fig** and **S8 Table**).

344 Although not subjected to statistical comparison, it may be useful to highlight observed
345 trends between map and painting viewing. On average, participants spent about twice as much
346 time viewing paintings compared to maps, as indexed by dwell time. This discrepancy may be
347 attributed to several factors: Participants might have found artworks more engaging than
348 climate crisis maps, or the smaller number of paintings (two) compared to maps (ten) could have
349 allowed for longer individual viewing times per painting. Additionally, the maps might not have
350 contained as much visual information or complexity, which might have required less time to
351 view. Another notable difference was also observed in average fixation duration, which was
352 highly shorter for painting viewing compared to map viewing. Longer average fixation
353 durations sometimes suggest a higher cognitive load, while shorter fixations might indicate that
354 the task of viewing paintings was less cognitively demanding, or that the information was easier
355 to process. This difference could also be influenced by methodological factors: fixation detection
356 algorithms might perform differently on screen-based stimuli versus in situ observation, with
357 the latter possibly affected by participant mobility during painting viewing. Lastly, in both
358 settings, fixation counts were higher in paired viewing conditions, indicating a consistent trend
359 across this metric. Interestingly, while dwell times were comparable between single and paired
360 map viewing conditions, they differed significantly in painting viewing, suggesting a minor
361 preferential difference between the two types of stimuli.

362 **4.3. Climate change anxiety scale (CCAS) responses**

363 Irrespective of the viewing condition, whether single or paired, the analysis of the
364 climate change anxiety scale involved four subscales of the 22-item questionnaire, with
365 responses gathered using a 5-point Likert scale. For a visual representation of the responses,

366 refer to **S8 Fig** for the frequency plot of individual items, **S9 Fig** for the aggregated frequency
367 plot across the four subscales, and **S9 Table** for a statistical breakdown.

368 Overall, levels of climate change anxiety were relatively low across the sample. For the
369 first two, often highly correlated subscales (cognitive-emotional impairment and functional
370 impairment), participants typically reported low scores. More than half of the responses were
371 “never,” and approximately a quarter were “rarely.” However, a small subset of participants
372 exhibited mid or high scores on these measures, suggesting notable levels of climate-related
373 anxiety for a minority of participants within the group.

374 Furthermore, responses on the personal experience with climate change subscale, and
375 more distinctly on the behavioural engagement subscale, were comparatively higher. While the
376 distribution of responses on the personal experience subscale was relatively even across all five
377 points of the Likert scale, the behavioural engagement subscale showed a negatively skewed
378 distribution. This suggests that on average, participants either exhibited or aspired to positive
379 behaviours towards addressing the climate crisis.

380 When investigating the relationships between the four subscales of the climate change
381 anxiety scale (CCAS), the 5-point Likert scale responses were treated as ordinal data, assigning
382 values from 0 (never) to 4 (almost always). Despite the frequency distributions varying across
383 the subscales, their relationships were examined through cross-correlation, using Spearman’s
384 rho and Kendall’s tau-b. These analyses showed positive linear correlations between the
385 subscales, as illustrated in **S10 Fig**, and detailed in **S10 Table**. This suggests that a combined
386 CCAS score could be formed as a cohesive construct for further analysis.

387 To explore the relationship between this aggregated CCAS score (treated as ordinal
388 data) and the four primary gaze metrics (treated as continuous data), we conducted correlation
389 analyses. The results, however, indicated no significant correlations; all relationships were
390 effectively flatlined across the metrics. This lack of significant findings implies that there is no

391 immediate or obvious connection between main gaze metrics and self-reported climate anxiety,
392 as detailed in **S11 Table**. Given these outcomes, we did not proceed further, such as dividing
393 participants into low and high anxiety groups based on median, quartile, or range-based splits.

394 **5. Discussion and Conclusions**

395 The present study established the relevance of using mobile eye-tracking to examine
396 how people look at climate change maps, and provided insights for scaling it up to more
397 naturalistic settings, notably social ones. Despite individual differences, on average, the
398 comparison between conditions during map viewing suggests that social interaction can subtly
399 alter gaze patterns. Paired viewing was associated with higher fixation counts, shorter average
400 fixation durations, and longer scanpaths, though dwell times remained comparable. These
401 variations may indicate differences in visual and cognitive processing, such as varying cognitive
402 efforts [30], or social motivation [31].

403 Attentional hotspots, indexed by fixation heatmaps, were broadly similar, indicating that
404 the content of visual stimuli primarily captures attention, often displaying a Euro-centric bias.
405 This implies that the bottom-up, object-based factors such as image saliency may have a larger
406 effect on viewing patterns. However, dissimilarities can be partially explained by how social
407 contexts shape viewer engagement, thereby influencing their information processing strategies.

408 Additionally, gaze metrics differed between viewing maps and artworks. Scientific
409 information processing and aesthetic perception showed some distinct viewing strategies, with
410 map viewing generally associated on average with longer fixation durations. These preliminary
411 findings align to some extent with prior work highlighted in the Introduction, suggesting that
412 viewing context (including differences between laboratory and museum environments) and the
413 authenticity of stimuli (such as reproductions versus originals) can influence gaze patterns and
414 overall engagement with visual stimuli. Although not directly comparable (given that this study

415 was conducted in a lab setting with reproductions of artworks), it is worth considering what
416 constitutes the genuine context for climate change maps, which are encountered in a variety of
417 settings.

418 Although there were significant positive linear cross-correlations among the subscales of
419 the CCAS, the lack of a significant linear correlation between main gaze metrics and climate
420 anxiety scores suggests that visual attention, as indexed by main gaze metrics, may not directly
421 relate to self-reported trait anxiety levels. It is important to note that no additional measures
422 were used to capture contextual emotional responses of participants to the content in this study.

423 The small size of the paired-viewing group, due to convenience sampling, and the
424 inherent data noise in mobile eye-tracking need to be considered when assessing these pilot
425 results. The imbalance between single- and paired-viewing conditions, as well as the limited
426 diversity in gender and age, further limits the generalisability of the findings. These constraints
427 reflect the challenges of recruiting larger, more balanced samples for mobile eye-tracking
428 studies, which typically require specialised equipment and substantial resources. Additionally,
429 participants might have treated the viewing differently within the experimental setting
430 compared to a naturalistic environment, such as a museum or classroom. Nonetheless, the
431 observed differences between isolated and social settings, and between maps and artworks, show
432 that the method can successfully capture differences in viewing patterns, even under these
433 conditions. This study provides a foundation for future research to consider the impact of
434 various types of climate-related visual stimuli on a broader audience. Extending this research to
435 more ecologically valid settings, as highlighted earlier, could help further clarify how real-world
436 contexts shape engagement with scientific and aesthetic stimuli. Additionally, integrating
437 momentary affective assessments and qualitative assessments in mixed-methods designs could
438 also provide deeper insights into the cognitive and emotional dimensions of viewer engagement.

439 Our study highlights the potential of mobile eye-tracking for understanding how people
440 engage with climate projections. Behavioural science has been hinted as a precious source of

441 recommendations to enhance climate visualisations in four key areas: how to direct visual
442 attention, reduce visual complexity, support inference-making, and integrate text with graphics
443 [1], and this study clearly demonstrates how it can contribute to the first objective. This should
444 not mean that the other aspects are equally essential and require further investigation. Visual
445 complexity and text-graphic integration can also be tested with eye-tracking and highlights
446 future uses for the methods. The reason not to pursue those here is that our approach aimed to
447 mimic everyday encounters with climate content by allowing participants to simply view images
448 naturally, without additional inference, understanding, or memory questions as in some other
449 research [32].

450 The differences in visual engagement between single and paired viewing conditions, as
451 well as between maps and artworks, underscore the potential for visual communication
452 strategies better tailored to contexts. Research indicates that changing graph designs derived
453 from IPCC reports can intentionally alter perceptions and even shift the credibility of the
454 presented data [33]. Strategies leveraging different media formats can enhance public
455 understanding of climate science. For instance, the memorability of visualisations [34] can be
456 utilised to promote climate action, with eye-tracking and visual attention serving as useful tools
457 to assess the effectiveness of different visualisations.

458 Although our study used static images, previous research has shown that interactive
459 visualisations that are more personally relevant yield promising results in terms of perceived
460 reality of climate change, attitude certainty, and concern [35]. Tailoring of communication can
461 also be done for different viewers. In the present case, we did not find evidence of differences
462 between individuals with different trait climate anxiety. Other directions remain open. For
463 instance, individuals with varying levels of optimism, when presented with climate change
464 messages in text, show different allocations of visual attention and recall, underlining attentional
465 bias and suggesting the need to redesign our communications [36]. Preliminary evidence also
466 suggests different viewing strategies and actions between political groups (liberals and

467 conservatives), highlighting the ideological influence on visual attention [37] and the need for
468 tailored communication tools to address such attentional and perceptual biases [38].

469 Behavioural sciences can play a crucial role in identifying and overcoming psychological
470 barriers to climate action [39]. However, creating effective interventions poses significant
471 challenges, as evidenced by large-scale cross-cultural studies [40]. Therefore, from a
472 methodological standpoint, employing behavioural data collection using mobile, screen-based,
473 or XR eye-tracking can be seen as essential for pinpointing visual attention, and later on help
474 for improving climate communication and interventions.

475 **6. Supplementary information**

476 **6.1. Data and code availability**

477 All anonymized data sets are publicly accessible for verification and reuse, in two
478 directories corresponding to maps and paintings: osf.io/2jqcu and osf.io/5bh78

479 **6.2. Acknowledgements**

480 The authors extend their gratitude to Prof Szonya Durant for providing access to the
481 RHUL VR Lab (Virtual Reality Laboratory, Department of Psychology, Royal Holloway,
482 University of London) as the data collection site; and to Dr Étienne Serbe-Kamp for the
483 valuable comments on the original draft.

484 **6.3. Authorship contribution statement**

485 Contributions of the authors are defined according to the CRediT (Contributor Roles
486 Taxonomy). **Doga Gulhan:** Conceptualization, Methodology, Software, Formal analysis,
487 Investigation, Data Curation, Writing - Original Draft, Writing - Review & Editing,

488 Visualisation. **Bahador Bahrami:** Writing - Review & Editing, Supervision, Project
489 administration, Funding acquisition. **Ophelia Deroy:** Writing - Review & Editing, Funding
490 acquisition.

491 **6.4. Competing interests**

492 The authors have declared that no competing interests exist.

493 **6.5. Funding statement**

494 We acknowledge support from Royal Holloway, University of London (RHUL) and
495 Ludwig Maximilian University of Munich (LMU) for providing salary and stipend
496 arrangements to the main author, Doga Gulhan. Partial funding for this project was provided
497 by a grant (ID: TRT-0480) from the Templeton Religion Trust (templetonreligiontrust.org),
498 titled “Aesthetic Cognitivism for Groups: Collective Ways of Looking and Sense-making”,
499 awarded to co-author Bahador Bahrami, and by a grant (ID: 10349) from the Volkswagen
500 Stiftung Grant (volkswagenstiftung.de), titled “Ways of Seeing, Ways of Knowing”, awarded to
501 co-author Ophelia Deroy. Bahador Bahrami was supported by the European Research Council
502 (ERC) under the European Union’s Horizon 2020 research and innovation programme
503 (819040 – acronym: rid-O). Ophelia Deroy was supported by the Volkswagen Stiftung
504 Momentum Grant (Co-Sense) and the additional module (Ways of Seeing). The funders did not
505 play any role in the study design, data collection and analysis, decision to publish, or preparation
506 of the manuscript.

507 **7. References**

- 508 [1] Harold J, Lorenzoni I, Shipley TF, Coventry KR. Cognitive and psychological science insights to improve
509 climate change data visualization. *Nat Clim Change* 2016;6:1080–9.
510 <https://doi.org/10.1038/nclimate3162>.

- 511 [2] Fish CS. Cartographic content analysis of compelling climate change communication. *Cartogr Geogr Inf*
512 [Sci](https://doi.org/10.1080/15230406.2020.1774421) 2020;47:492–507. <https://doi.org/10.1080/15230406.2020.1774421>.
- 513 [3] Morelli A, Johansen TG, Pidcock R, Harold J, Pirani A, Gomis M, et al. Co-designing engaging and
514 accessible data visualisations: a case study of the IPCC reports. *Clim Change* 2021;168:26.
515 <https://doi.org/10.1007/s10584-021-03171-4>.
- 516 [4] Wardekker A, Lorenz S. The visual framing of climate change impacts and adaptation in the IPCC
517 assessment reports. *Clim Change* 2019;156:273–92. <https://doi.org/10.1007/s10584-019-02522-6>.
- 518 [5] Steinke TR. Eye Movement Studies In Cartography And Related Fields. *Cartogr Int J Geogr Inf*
519 [Geovisualization](https://doi.org/10.3138/J166-635U-7R56-X2L1) 1987;24:40–73. <https://doi.org/10.3138/J166-635U-7R56-X2L1>.
- 520 [6] Dong W, Liao H, Xu F, Liu Z, Zhang S. Using eye tracking to evaluate the usability of animated maps. *Sci*
521 [China Earth Sci](https://doi.org/10.1007/s11430-013-4685-3) 2014;57:512–22. <https://doi.org/10.1007/s11430-013-4685-3>.
- 522 [7] Ooms K, De Maeyer P, Fack V. Study of the attentive behavior of novice and expert map users using eye
523 tracking. *Cartogr Geogr Inf Sci* 2014;41:37–54. <https://doi.org/10.1080/15230406.2013.860255>.
- 524 [8] Kiefer P, Giannopoulos I, Raubal M. Where Am I? Investigating Map Matching During Self-Localization
525 With Mobile Eye Tracking in an Urban Environment. *Trans GIS* 2014;18:660–86.
526 <https://doi.org/10.1111/tgis.12067>.
- 527 [9] Netzel R, Ohlhausen B, Kurzhals K, Woods R, Burch M, Weiskopf D. User performance and reading
528 strategies for metro maps: An eye tracking study. *Spat Cogn Comput* 2017;17:39–64.
529 <https://doi.org/10.1080/13875868.2016.1226839>.
- 530 [10] Göbel F, Kiefer P, Raubal M. FeaturEyeTrack: automatic matching of eye tracking data with map features
531 on interactive maps. *GeoInformatica* 2019;23:663–87. <https://doi.org/10.1007/s10707-019-00344-3>.
- 532 [11] Liao H, Wang X, Dong W, Meng L. Measuring the influence of map label density on perceived complexity:
533 a user study using eye tracking. *Cartogr Geogr Inf Sci* 2019;46:210–27.
534 <https://doi.org/10.1080/15230406.2018.1434016>.
- 535 [12] Keskin M, Ooms K, Dogru AO, De Maeyer P. Exploring the Cognitive Load of Expert and Novice Map
536 Users Using EEG and Eye Tracking. *ISPRS Int J Geo-Inf* 2020;9:429.
537 <https://doi.org/10.3390/ijgi9070429>.
- 538 [13] Döll P. Cartograms Facilitate Communication of Climate Change Risks and Responsibilities. *Earths Future*
539 2017;5:1182–95. <https://doi.org/10.1002/2017EF000677>.
- 540 [14] Terrado M, Calvo L, Christel I. Towards more effective visualisations in climate services: good practices
541 and recommendations. *Clim Change* 2022;172:18. <https://doi.org/10.1007/s10584-022-03365-4>.

- 542 [15] Budescu DV, Por H-H, Broomell SB, Smithson M. The interpretation of IPCC probabilistic statements
543 around the world. *Nat Clim Change* 2014;4:508–12. <https://doi.org/10.1038/nclimate2194>.
- 544 [16] Battocletti V, Romano A, Sotis C. People can understand IPCC visuals and are not influenced by colors.
545 *Environ Res Lett* 2023;18:114036. <https://doi.org/10.1088/1748-9326/acfb95>.
- 546 [17] Schneider B, Nocke T. The Feeling of Red and Blue—A Constructive Critique of Color Mapping in Visual
547 Climate Change Communication. In: Leal Filho W, Manolas E, Azul AM, Azeiteiro UM, McGhie H,
548 editors. *Handb. Clim. Change Commun.* Vol 2, Cham: Springer International Publishing; 2018, p. 289–
549 303. https://doi.org/10.1007/978-3-319-70066-3_19.
- 550 [18] Cramer F, Shephard GE, Heron PJ. The misuse of colour in science communication. *Nat Commun*
551 2020;11:5444. <https://doi.org/10.1038/s41467-020-19160-7>.
- 552 [19] Locher P, Smith L, Smith J. Original Paintings versus Slide and Computer Reproductions: A Comparison
553 of Viewer Responses. *Empir Stud Arts* 1999;17:121–9. <https://doi.org/10.2190/R1WN-TAF2-376D-EFUH>.
- 555 [20] Brieber D, Leder H, Nadal M. The Experience of Art in Museums: An Attempt to Dissociate the Role of
556 Physical Context and Genuineness. *Empir Stud Arts* 2015;33:95–105.
557 <https://doi.org/10.1177/0276237415570000>.
- 558 [21] Brieber D, Nadal M, Leder H. In the white cube: Museum context enhances the valuation and memory of
559 art. *Acta Psychol (Amst)* 2015;154:36–42. <https://doi.org/10.1016/j.actpsy.2014.11.004>.
- 560 [22] Grüner S, Specker E, Leder H. Effects of Context and Genuineness in the Experience of Art. *Empir Stud*
561 *Arts* 2019;37:138–52. <https://doi.org/10.1177/0276237418822896>.
- 562 [23] Reitstätter L, Brinkmann H, Santini T, Specker E, Dare Z, Bakondi F, et al. The display makes a difference:
563 A mobile eye tracking study on the perception of art before and after a museum’s rearrangement. *J Eye*
564 *Mov Res* 2020;13. <https://doi.org/10.16910/jemr.13.2.6>.
- 565 [24] Gulhan D, Durant S, Zanker JM. Similarity of gaze patterns across physical and virtual versions of an
566 installation artwork. *Sci Rep* 2021;11:18913. <https://doi.org/10.1038/s41598-021-91904-x>.
- 567 [25] Specker E, Arató J, Leder H. How are real artworks and reproductions judged? The role of anchoring in
568 empirical investigations of the genuineness effect. *J Exp Soc Psychol* 2023;108:104494.
569 <https://doi.org/10.1016/j.jesp.2023.104494>.
- 570 [26] Mauritshuis Museum, Neurensics, Neurofactor. The unconscious emotions that art evokes: Neuroscience
571 research into the impact of a museum visit (Final Report). 2024.

- 572 [27] Iturbide M, Fernández J, Gutiérrez JM, Bedia J, Cimadevilla E, Díez-Sierra J, et al. Repository supporting
573 the implementation of FAIR principles in the IPCC-WGI Atlas 2021.
574 <https://doi.org/10.5281/ZENODO.3691645>.
- 575 [28] Intergovernmental Panel On Climate Change (Ipcc). Climate Change 2021 – The Physical Science Basis:
576 Working Group I Contribution to the Sixth Assessment Report of the Intergovernmental Panel on
577 Climate Change. 1st ed. Cambridge University Press; 2023. <https://doi.org/10.1017/9781009157896>.
- 578 [29] Clayton S, Karazsia BT. Development and validation of a measure of climate change anxiety. *J Environ*
579 *Psychol* 2020;69:101434. <https://doi.org/10.1016/j.jenvp.2020.101434>.
- 580 [30] Chen S, Epps J, Ruiz N, Chen F. Eye activity as a measure of human mental effort in HCI. *Proc. 16th Int.*
581 *Conf. Intell. User Interfaces*, Palo Alto CA USA: ACM; 2011, p. 315–8.
582 <https://doi.org/10.1145/1943403.1943454>.
- 583 [31] Deroy O, Longin L, Bahrami B. Co-perceiving: Bringing the social into perception. *WIREs Cogn Sci*
584 2024:e1681. <https://doi.org/10.1002/wcs.1681>.
- 585 [32] Šašinka Č, Stachoň Z, Čeněk J, Šašinková A, Popelka S, Ugwitz P, et al. A comparison of the performance
586 on extrinsic and intrinsic cartographic visualizations through correctness, response time and cognitive
587 processing. *PLOS ONE* 2021;16:e0250164. <https://doi.org/10.1371/journal.pone.0250164>.
- 588 [33] Courtney SL, McNeal KS. Seeing is believing: Climate change graph design and user judgments of
589 credibility, usability, and risk. *Geosphere* 2023;19:1508–27. <https://doi.org/10.1130/GES02517.1>.
- 590 [34] Borkin MA, Vo AA, Bylinskii Z, Isola P, Sunkavalli S, Oliva A, et al. What Makes a Visualization
591 Memorable? *IEEE Trans Vis Comput Graph* 2013;19:2306–15.
592 <https://doi.org/10.1109/TVCG.2013.234>.
- 593 [35] Herring J, VanDyke MS, Cummins RG, Melton F. Communicating Local Climate Risks Online Through
594 an Interactive Data Visualization. *Environ Commun* 2017;11:90–105.
595 <https://doi.org/10.1080/17524032.2016.1176946>.
- 596 [36] Beattie G, Marselle M, McGuire L, Litchfield D. Staying over-optimistic about the future: Uncovering
597 attentional biases to climate change messages. *Semiotica* 2017;2017:21–64. <https://doi.org/10.1515/semt-2016-0074>.
- 599 [37] Luo Y, Zhao J. Motivated Attention in Climate Change Perception and Action. *Front Psychol*
600 2019;10:1541. <https://doi.org/10.3389/fpsyg.2019.01541>.
- 601 [38] Luo Y, Zhao J. Attentional and perceptual biases of climate change. *Curr Opin Behav Sci* 2021;42:22–6.
602 <https://doi.org/10.1016/j.cobeha.2021.02.010>.

603 [39] Van Der Linden S, Weber EU. Editorial overview: Can behavioral science solve the climate crisis? Curr
604 Opin Behav Sci 2021;42:iii–viii. <https://doi.org/10.1016/j.cobeha.2021.09.001>.
605 [40] Vlasceanu M, Doell KC, Bak-Coleman JB, Todorova B, Berkebile-Weinberg MM, Grayson SJ, et al.
606 Addressing climate change with behavioral science: A global intervention tournament in 63 countries. Sci
607 Adv 2024;10:eadj5778. <https://doi.org/10.1126/sciadv.adj5778>.
608

609 **8. Supporting information**

610 **S1 Fig. Overview of main stimuli: ten climate crisis maps.**
611 **S2 Fig. Overview of supplementary stimuli: two paintings.**
612 **S3 Fig. Data recording setup.**
613 **S4 Fig. Procedure diagram for viewing ten maps.**
614 **S5 Fig. Online data pre-processing using MME and RIM methods.**
615 **S6 Fig. Breakdown of box plots of descriptive statistics for main gaze metrics by**
616 **map.**
617 **S7 Fig. Breakdown of box plots of descriptive statistics for main gaze metrics by**
618 **painting.**
619 **S8 Fig. Frequency plot of survey results, item-wise.**
620 **S9 Fig. Frequency plots of survey results, by four subcategories.**
621 **S10 Fig. Correlation plots between four subscales of the CCAS.**
622 **S1 Table. Gaze metrics for maps.**
623 **S2 Table. Nonparametric ANOVA (Kruskal-Wallis test) for maps, comparing**
624 **single and paired viewing conditions.**
625 **S3 Table. Gaze metrics for maps, broken down by projection timeframe and**
626 **type.**
627 **S4 Table. Gaze metrics for maps, fully broken down.**

- 628 **S5 Table. Gaze metrics for maps divided into two AOIs.**
- 629 **S6 Table. Gaze metrics for paintings.**
- 630 **S7 Table. Nonparametric ANOVA (Kruskal-Wallis test) for paintings, comparing**
631 **single and paired viewing conditions.**
- 632 **S8 Table. Gaze metrics for paintings, fully broken down.**
- 633 **S9 Table. Survey descriptive statistics by CCAS subscales.**
- 634 **S10 Table. Survey correlation statistics for CCAS subscales.**
- 635 **S11 Table. Correlations between gaze metrics and total CCAS score.**
- 636 **S1 File. The Climate Change Anxiety Scale (CCAS).**

1 **I. Supplementary materials**

2 Studying attention to IPCC climate change maps with mobile eye-
3 tracking

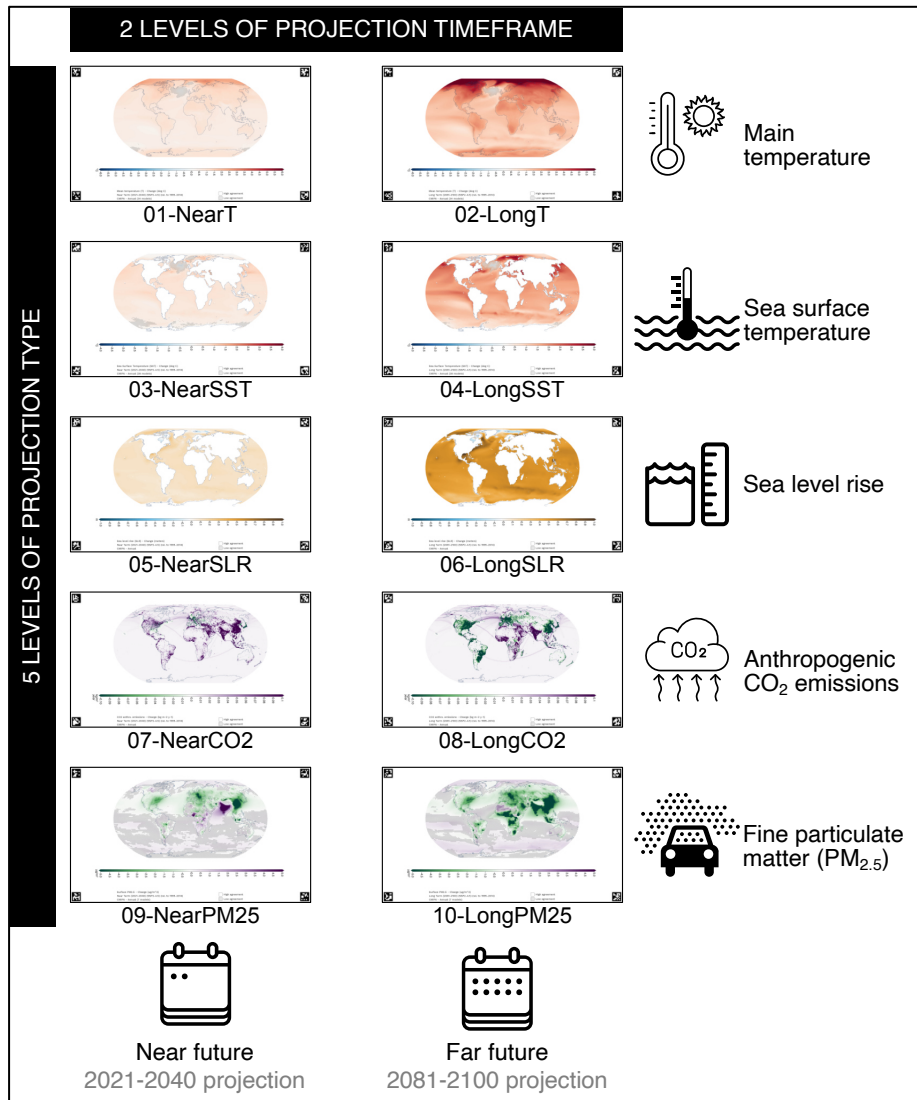
4 Doga Gulhan^{*,1,2}, Bahador Bahrami², Ophelia Deroy³

5 ¹Department of Psychology, Royal Holloway, University of London, UK

6 ²Faculty of General Psychology and Education, Ludwig Maximilian University of Munich, Germany

7 ³Faculty of Philosophy, Philosophy of Science and the Study of Religion, Ludwig Maximilian University of Munich,
8 Germany

9 *Corresponding author contact information: dogagulhan@gmail.com (DG)



10 **SI Fig. Overview of main stimuli: ten climate crisis maps.**

11 This figure provides an infographic overview of the main stimuli, consisting of five pairs of world maps with a
 12 Robinson projection. These maps were generated using the online data visualisation tool from the
 13 Intergovernmental Panel on Climate Change (IPCC) and downloaded from their website (ipcc.ch and interactive-atlas.ipcc.ch). Each map features a heatmap overlay representing a specific type of climate projection, accompanied
 14 by a relevant scale and brief data description below it. The maps are organised into two columns representing
 15 different projection timeframes: the near future (2021-2040) and the far future (2081-2100), with corresponding
 16 icons beneath for illustrative purposes. The five rows depict different projection types: temperature change in °C,
 17 sea surface temperature change in °C, sea level rise in metres, anthropogenic CO₂ emissions in kg/m² per year,
 18 and particulate matter (PM_{2.5}) concentration changes in µg/m³, with icons on the right for illustration. In the
 19 experiment, these maps were displayed full-screen on a 17-inch laptop monitor. Each map presentation was
 20 preceded by a title card (not shown here) that displayed these icons and titles, informing participants about the
 21 content of the upcoming map. A countdown from 30 seconds and a brief instruction text afterwards (not illustrated
 22 here) were also present during each trial, indicating that participants could advance to the next map at any time
 23 by pressing the spacebar. Below the maps, naming conventions are listed, which are used in subsequent data
 24 visualisations like bar plots in this paper. Note that small Apriltags around each map were initially intended for the
 25 Marker Mapper (MM) preprocessing pipeline but were not used, as the Reference Image Mapper (RIM)
 26 preprocessing pipeline was used instead, which does not require Apriltags. (See Methods for details).

27

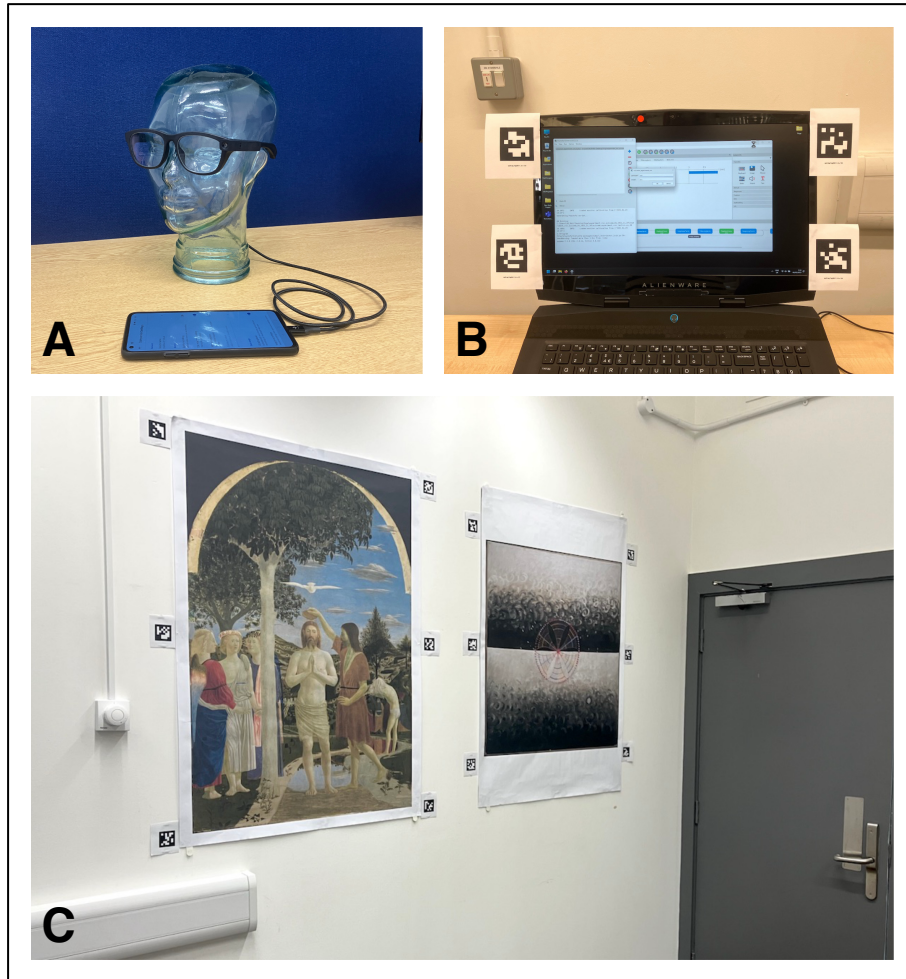


28

S2 Fig. Overview of supplementary stimuli: two paintings.

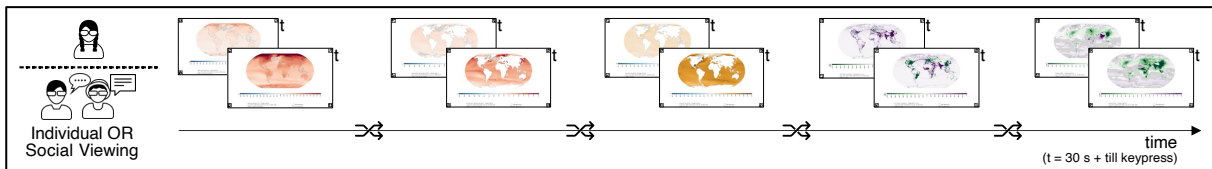
29

This figure showcases high-resolution digital images of two paintings printed on A0-sized posters, serving as a small supplementary stimulus set. These paintings were selected for their distinct content and downloaded from Wikimedia Commons (commons.wikimedia.org). **Top-left (a):** The Baptism of Christ by Piero della Francesca, completed circa 1448–50, actual size approximately 167 cm × 116 cm. **Top-right (b):** The Swan, No. 10, by Hilma af Klint, completed in 1915, actual size approximately 150 cm × 150 cm. **Bottom-left (c)** and **Bottom-right (d)** feature photographs of the original artworks as seen at the National Gallery, London, and Tate Modern, London, respectively, photographed by DG.



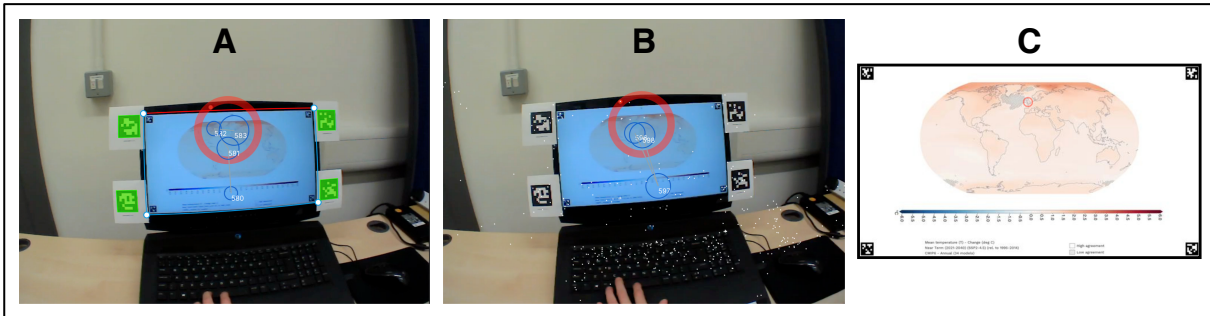
36 **S3 Fig. Data recording setup.**

37 **Top-left (a):** For gaze data collection, the mobile eye-tracker (Pupil Invisible) was attached to a companion
 38 recording device (OnePlus 8 Android phone) running the Pupil Invisible Companion App. Gaze data were
 39 collected at 200 Hz with a resolution of 192×192 pixels using two near-eye cameras with infrared illumination.
 40 Scene videos were recorded at 30 Hz with a resolution of 1088×1080 pixels, roughly corresponding to an $82^\circ \times$
 41 82° field of vision. **Top-right (b):** The laptop used (Dell Alienware 17 – 2019) displayed the maps and collected
 42 responses for the climate scale task and exit questionnaire. It featured a screen resolution of 1920×1080 pixels
 43 and a diagonal size of 17.3 inches (~44 cm), set in a 16:9 aspect ratio (~ 38×21.5 cm display dimensions). Although
 44 participants sat at a regular work desk, the distance from screen to participant varied and was not controlled;
 45 however, it is approximately noted that at an average distance of 57 cm, 1 cm on the screen roughly equates to 1
 46 degree of visual angle. **Bottom (c):** Two artwork posters were displayed side by side in the lab, colour-printed on
 47 A0 papers (841×1189 mm) with a white border and surrounded by six April tags for positional referencing. For
 48 further technical details on April tags and their implementations in the Pupil Cloud, Pupil Cloud data streams,
 49 marker mapper and reference image mapper enrichments, see the following resources:
 50 <https://april.eecs.umich.edu/software/apriltag>
 51 <https://docs.pupil-labs.com/core/software/pupil-capture/#markers>
 52 <https://docs.pupil-labs.com/invisible/basic-concepts/data-streams/>
 53 [https://docs.pupil-labs.com/enrichments\(marker-mapper/](https://docs.pupil-labs.com/enrichments(marker-mapper/)
 54 <https://docs.pupil-labs.com/enrichments/reference-image-mapper/>



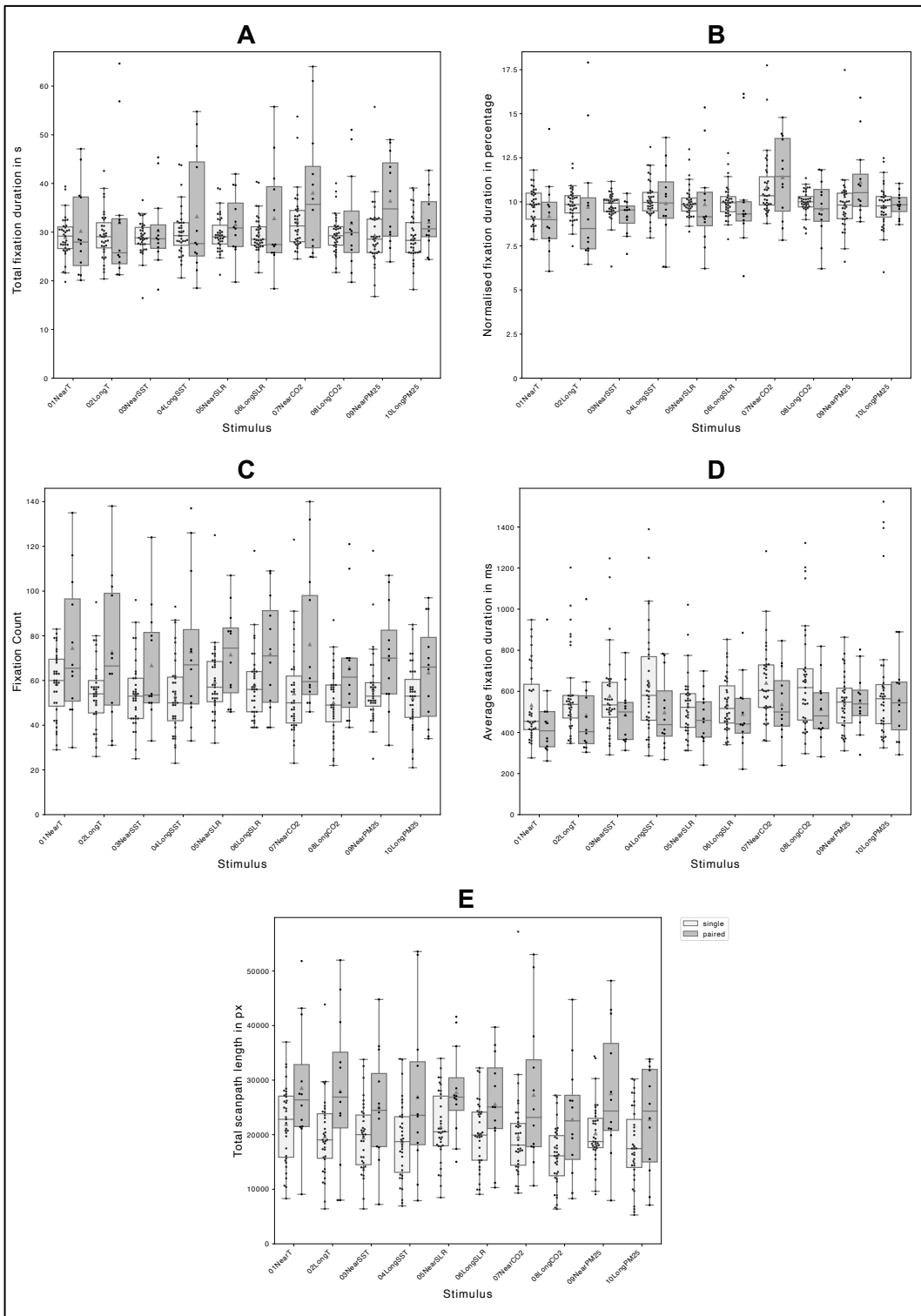
55 **S4 Fig. Procedure diagram for viewing ten maps.**

56 This diagram illustrates the time-course of viewing conditions for both individual and paired participants.
 57 Participants viewed the complete set of ten maps in a pairwise randomised order, starting with the near-future
 58 version followed by the far-future version of the same projection type. Each map was displayed for a minimum of
 59 30 seconds, after which a small description appeared at the top, allowing participants to view the map as long as
 60 desired until proceeding to the next by pressing a spacebar key. Before any map presentation, a brief title screen
 61 (lasting approximately five seconds) introduced the content of the upcoming map with a couple of words and two
 62 icons (similar to those in Figure 1). In paired viewing conditions, participants were encouraged to discuss the maps
 63 if desired, although this varied among pairs. Each map remained visible until the group chose to proceed, provided
 64 at least 30 seconds had elapsed. The sequence of map presentations was randomised in pairs, with $N_{\text{Stimulus}} = 10$ as
 65 five pairs of near- and far-future projections. Note that a similar procedure was employed for viewing the two
 66 paintings (not illustrated here for succinctness), with participants deciding the order and duration of viewing for
 67 the printed posters.



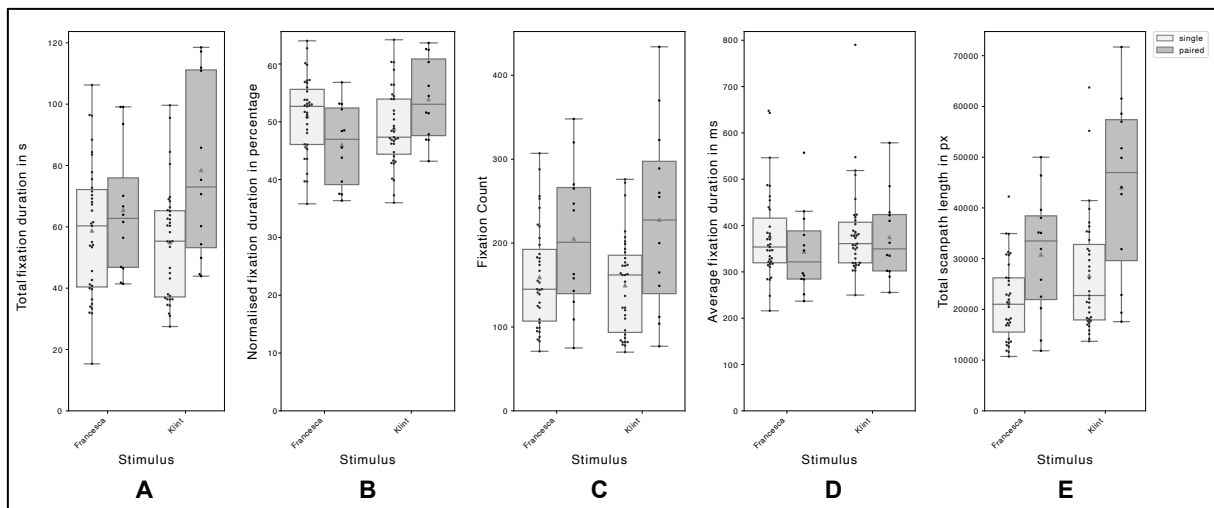
68 **S5 Fig. Online data pre-processing using MME and RIM methods.**

69 This figure demonstrates the two data processing methods used within Pupil Cloud for both screen-based (maps)
70 and in-situ (paintings) stimuli. **Left (a):** The Marker Mapper Enrichment (MME) method involved placing four
71 markers around the laptop screen (highlighted in green). The boundaries defined by these markers (shown with
72 blue and red borders) depict the surface within which raw gaze data are normalised. However, this method was
73 later abandoned due to relatively low data accuracy. **Middle (b):** The Reference Image Mapper (RIM) method
74 required separate scanning recordings lasting about one minute and snapshot images for each stimulus. It employs
75 a structure-from-motion technique to create a digital model from the video frames, shown as white dots
76 superimposed on the scene camera view. The raw gaze data are then normalised against this model and the
77 reference snapshot. Due to its relatively higher data accuracy, only data processed via RIM was used for analysis.
78 **Right (c):** This panel shows the process of normalising raw gaze data against the model and reference image,
79 where the red circle denotes the normalised location of the fixation with normalised XY coordinates relative to the
80 pixels of the snapshot image. Note that the same preprocessing methods were applied to the supplementary
81 painting stimuli (not shown here for brevity).



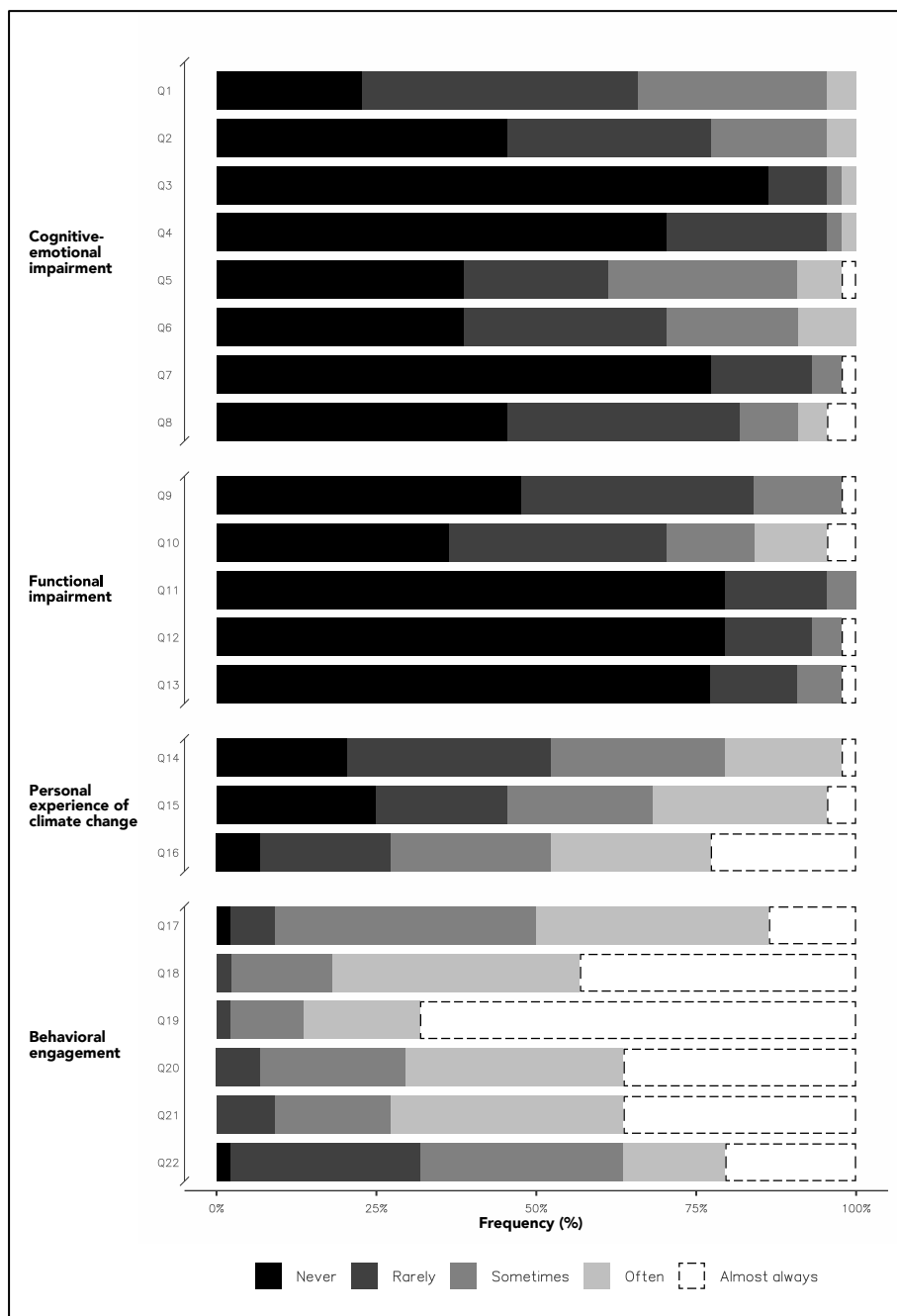
82 **S6 Fig. Breakdown of box plots of descriptive statistics for main gaze metrics by map.**

83 Supplementing the cumulative box plots, this figure details the breakdown of gaze metrics for ten individual maps.
 84 It follows the same format as the previous figure, presenting metrics for: **(a)** total fixation duration in milliseconds,
 85 **(b)** normalised fixation duration as a percentage (dwell time), **(c)** fixation count, **(d)** average fixation duration in
 86 milliseconds, and **(e)** total proxy scanpath length in pixels. Box plots are colour-coded in light and dark greys to
 87 represent single- ($N_{\text{StimulusSingle}} = 35$) and paired-viewing ($N_{\text{StimulusPaired}} = 12$) conditions, respectively. Each box plot
 88 shows the range (excluding outliers), IQR, median, and mean (marked with a small triangle). The categorical x-
 89 axis categorises the ten maps as different stimuli, while the y-axis denotes each metric. Scanpath distances are
 90 calculated similar to the previous figure.



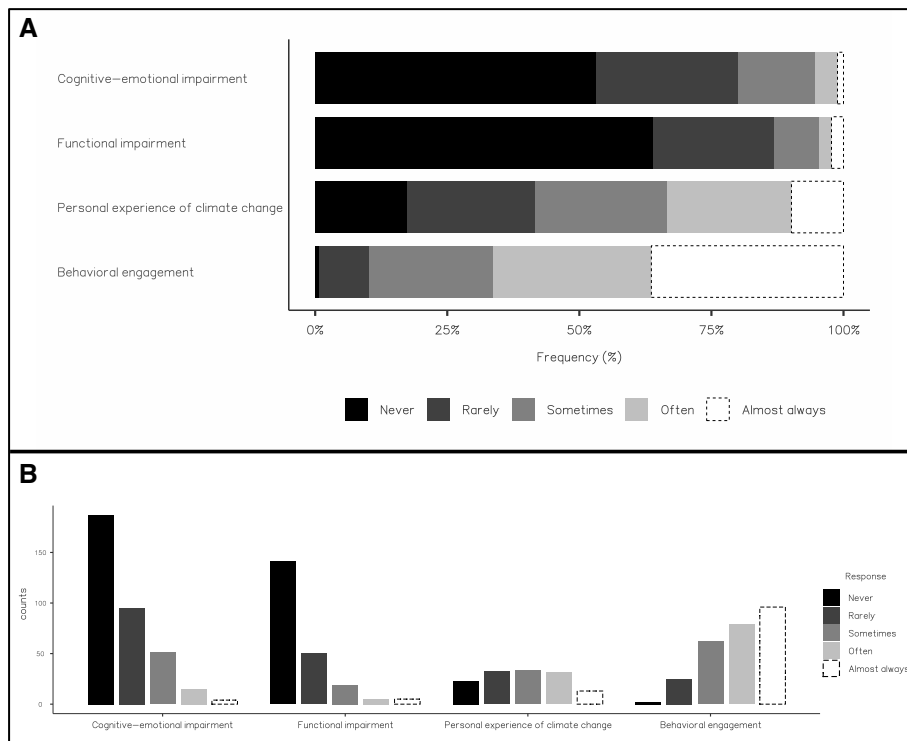
S7 Fig. Breakdown of box plots of descriptive statistics for main gaze metrics by painting.

This figure supplements the cumulative box plots by detailing the breakdown of gaze metrics for two individual paintings. It showcases the same five main gaze metrics: **(a)** total fixation duration in milliseconds (dwell time), **(b)** normalised fixation duration as a percentage, **(c)** fixation count, **(d)** average fixation duration in milliseconds, and **(e)** total proxy scanpath length in pixels. The box plots are colour-coded in light and dark greys to distinguish between single-viewing ($N_{\text{SampleSingle}} = 35$, $N_{\text{StimulusSingle}} = 35$) and paired-viewing ($N_{\text{SamplePaired}} = 12$, $N_{\text{StimulusPaired}} = 12$) conditions, as described in the legend at the top right. Each plot displays the range (excluding outliers), interquartile range (IQR), median, and mean (indicated by a small triangle overlay), providing a detailed view of the variability. Data points within each plot reflect the values of individual stimuli, hence these are the broken-down box plots corresponding to each painting. Note that the proxy scanpath distances, calculated for both viewing conditions, are the cumulative sums of the Euclidean distances between two consecutive fixations for each painting and participant. These distances are based on the arbitrary pixel values from the reference images used for each painting: 685×1000 pixels for The Baptism of Christ (Painting #1) and 983×1000 pixels for The Swan (Painting #2), which introduces some compatibility issues in unified analysis, and requires further normalisation. The categorical x-axis denotes the two different paintings as stimuli, while the y-axis denotes each gaze metric.



106 **S8 Fig. Frequency plot of survey results, item-wise.**

107 This frequency table presents the aggregated responses from the Climate Change Anxiety Scale (refer to
108 Supplementary Material 1). The survey was conducted on a 5-point Likert scale across 22 items and presented
109 here irrespective of single or paired viewing conditions. Responses are colour-coded from black to white,
110 corresponding to the frequency from “never” to “almost always”, as shown in the legend below the table. The
111 scale includes four sub-scales, each associated with a set of questions: cognitive-emotional impairment (questions
112 1-8), functional impairment (questions 9-13), personal experience of climate change (questions 14-16), and
113 behavioural engagement (questions 17-22). These sub-scales are labelled on the left side of the frequency plot. Note
114 that $N_{\text{sample}} = 44$, as responses from three participants were not recorded.

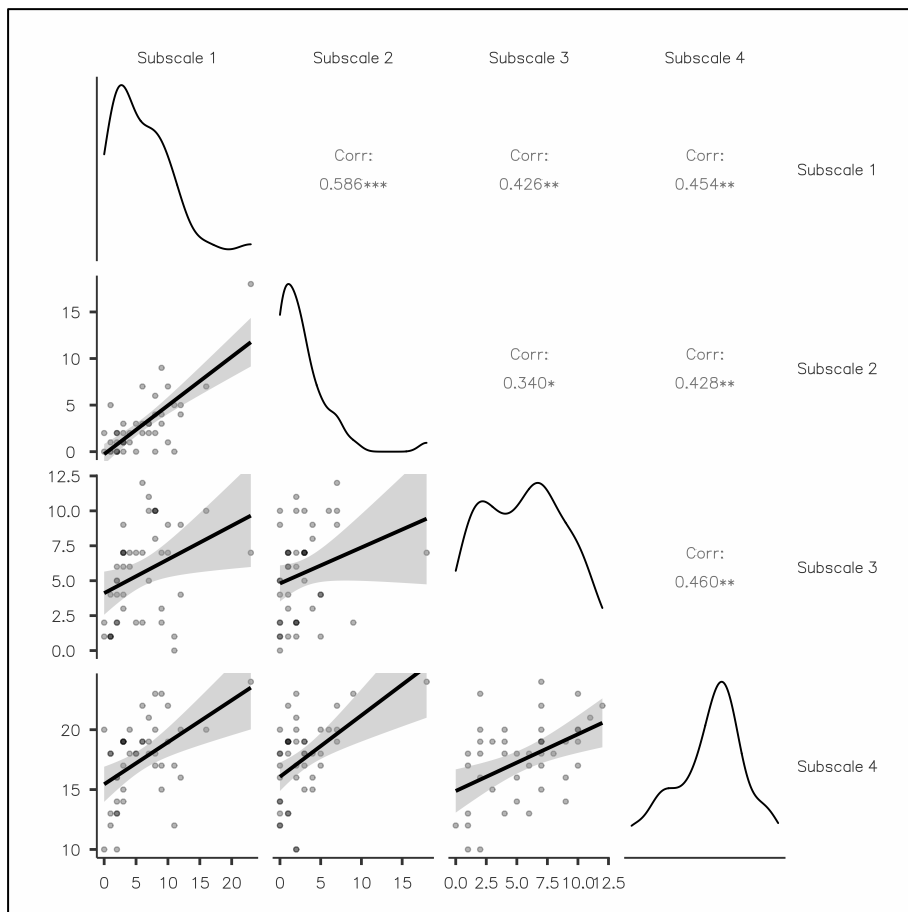


115

S9 Fig. Frequency plots of survey results, by four subcategories.

116

This figure displays the cumulative frequency table, aggregating responses into four sub-categories to show overall trends and frequency distributions within the Climate Change Anxiety Scale: **(a)** Four sub-categories plotted along a frequency X-axis, and **(b)** the same four subcategories visualised as count-based data, reflecting the differing number of questions per sub-scale. The y-axis counts reflect the total number of individual responses, varying by the number of questions in each sub-category: 8 questions under cognitive-emotional impairment, 5 under functional impairment, 3 under personal experience of climate change, and 6 under behavioural engagement. With $N_{\text{sample}} = 44$ due to three unrecorded participant responses, the total N_{Count} for responses are: 353 for cognitive-emotional impairment, 220 for functional impairment, 225 for personal experience, and 264 for behavioural engagement. The 5-point Likert scale is colour-coded from black to white, as shown in the accompanying legends.



126

S10 Fig. Correlation plots between four subscales of the CCAS.

127

This figure presents the cross-correlation between the four subscales of the Climate Change Anxiety Scale (CCAS). Labels at the top and right (from Subscale 1 to Subscale 4) correspond to the four subscales of the CCAS. Along the diagonal axis from top-left to bottom-right, the graphs display the response distribution for each subscale, where 5-point Likert scale data for each question (treated as ordinal data) is converted to 0-4 scores. Below the diagonal, six correlation plots reveal all possible pairwise correlations among the subscales. Each plot includes individual data points, a linear correlation line, and confidence intervals for visual guidance. Above the diagonal, the corresponding areas display the Spearman's rho correlation coefficients for each pair of subscales. Note that the sample size for these analyses was $N_{\text{Sample}} = 44$.

Descriptives						
	Condition	Total fixation duration in s	Normalised fixation duration in percentage	Fixation count	Average fixation duration in ms	Total scanpath length in px
N	single	350	350	350	350	350
	paired	120	120	120	120	120
Mean	single	29.7	10	55.12	586.43	19534.89
	paired	32.92	10	70.7	504.45	26288.61
Std. error mean	single	0.26	0.06	0.87	11.29	365.87
	paired	0.93	0.21	2.47	15.29	1036.95
Median	single	29.02	9.95	54	546.19	19280.35
	paired	29.45	9.68	65.5	479.26	25215.88
Standard deviation	single	4.81	1.2	16.2	211.18	6844.86
	paired	10.24	2.29	27.09	167.5	11359.19
Minimum	single	16.45	6.01	21	276.2	5285.11
	paired	18.19	5.78	30	221.36	7104.28
Maximum	single	55.73	17.75	125	1523	57201.18
	paired	64.65	17.91	140	1048.9	53560.01

135 **SI Table. Gaze metrics for maps.**

136 This table presents descriptive statistics for five gaze metrics observed while viewing maps: total fixation duration
 137 (in seconds and as a percentage of total viewing time), fixation count, average fixation duration (in milliseconds),
 138 and total proxy scanpath length in pixels. The metrics are reported with the following statistics for each:
 139 observation size (N), mean (M), standard deviation (SD), standard error of the mean (SEM), minimum (Min), and
 140 maximum (Max) values. The data ($N_{MapStimulus} = 10$) are segmented into single ($N_{SingleSample} = 35$) and paired
 141 ($N_{PairedSample} = 12$) viewing conditions, allowing for a direct comparison of these metrics under different social
 142 viewing contexts.

Kruskal-Wallis				
	χ^2	df	p	ϵ^2
Total fixation duration in s	1.7	1	0.193	0
Normalised fixation duration in percentage	3.22	1	0.073	0.01
Fixation count	28.69	1	<.001	0.06
Average fixation duration in ms	15.65	1	<.001	0.03
Total scanpath length in px	38.27	1	<.001	0.08

143 **S2 Table. Nonparametric ANOVA (Kruskal-Wallis test) for maps, comparing single and**
 144 **paired viewing conditions.**

145 This table details the results of a nonparametric ANOVA (Kruskal-Wallis test) used to analyse the differences in
 146 gaze metrics between single and paired viewing conditions for maps. Despite the exploratory nature of the research
 147 and the relatively low sample sizes ($N = 35$ for single and $N = 12$ for paired), significant differences were observed
 148 in fixation count, average fixation duration, and scanpath length, while no significant differences were found in
 149 total fixation duration. The table provides a detailed breakdown of the test results for each metric, including the
 150 chi-squared (χ^2) values, degrees of freedom (df), p-values, and effect sizes (ϵ^2). Note, although there is not a consensus
 151 on effect size interpretation, $\epsilon^2 < .08$ may be assumed to be small, $\epsilon^2 < .26$ assumed to be medium, $\epsilon^2 \geq .26$
 152 assumed to be large.

A - Descriptives

		Projection timeframe	Total fixation duration in s	Normalised fixation duration in percentage	Fixation count	Average fixation duration in ms	Total scanpath length in px
Mean	Near	30.74	10.08	60.51	548.73	22296.16	
	Long	30.31	9.92	57.69	582.27	20222.32	
Std. error mean	Near	0.44	0.11	1.35	11.31	561.84	
	Long	0.44	0.1	1.35	14.98	570.83	
Median	Near	29.15	9.88	56	519.62	21093.2	
	Long	29	9.89	55	540.36	19544.69	
Standard deviation	Near	6.78	1.64	20.65	173.35	8612.78	
	Long	6.76	1.46	20.66	229.64	8750.73	

B - Descriptives

		Projection type	Total fixation duration in s	Normalised fixation duration in percentage	Fixation count	Average fixation duration in ms	Total scanpath length in px
Mean	T	29.73	9.73	60.9	535.54	22749.26	
	SST	30.13	9.85	57.8	578.21	20921.01	
	SLR	30.32	10	62.15	519.15	22296.17	
	CO2	31.98	10.45	57.09	617.88	19704.69	
	PM25	30.47	9.97	57.55	576.73	20625.08	
	T	0.73	0.17	2.24	20.16	969.22	
	SST	0.67	0.13	2.22	22.92	924.52	
	SLR	0.58	0.16	1.93	14.86	759.54	
	CO2	0.8	0.17	2.33	22.09	963.33	
	PM25	0.69	0.16	1.91	22.91	852.72	
Median	T	28.41	9.8	58.5	487.4	22221.5	
	SST	28.8	9.84	53	530.67	20033.92	
	SLR	28.94	9.84	58	497.18	21146.47	
	CO2	30.16	10.14	54.5	590.5	17778.25	
	PM25	29.05	9.91	54.5	550.93	19390.62	
Standard deviation	T	7.08	1.63	21.69	195.44	9396.89	
	SST	6.49	1.22	21.51	222.26	8963.56	
	SLR	5.58	1.59	18.68	144.12	7363.99	
	CO2	7.77	1.66	22.63	214.19	9339.81	
	PM25	6.65	1.56	18.5	222.12	8267.46	

153 **S3 Table. Gaze metrics for maps, broken down by projection timeframe and type.**

154 This table extends the analysis of cumulative gaze metrics by breaking down the data into either two projection
 155 timeframes or five projection types. It presents the same five metrics using mean (M), median, standard deviation
 156 (SD), and standard error of the mean (SEMs) without distinguishing between single or paired viewing conditions
 157 for brevity. **Top (a)** As projection timeframe breakdown, metrics are categorised into short-term (2021-2040) and
 158 long-term (2081-2100) projections. The observation count for each category is based on five times the total sample
 159 size ($N_{\text{sample}} = 47$), resulting in $N_{\text{Observations}} = 235$ for each timeframe, as in each cell value. **Bottom (b)** As projection
 160 type breakdown, metrics are detailed for five types of projections: main temperature (T), sea surface temperature
 161 (SST), sea level rise (SLR), anthropogenic CO₂ emissions (CO2), and fine particulate matter PM_{2.5} (PM25). The
 162 observation count for each type is based on twice the total sample size, resulting in $N_{\text{Observations}} = 94$ for each type,
 163 as in each cell value.

Descriptives								
			Total fixation duration in s	Normalised fixation duration in percentage	Fixation count	Average fixation duration in ms	Total scanpath length in px	
Mean	01NearT	single	29.01	9.77	58.6	533.67	21988.47	
		paired	30.29	9.21	74.58	451.1	28576.68	
	02LongT	single	29.44	9.88	54.46	583.67	19699.17	
		paired	32.07	9.72	72.75	485.04	28036.92	
	03NearSST	single	28.94	9.75	54.23	578.82	19499.82	
		paired	30.37	9.19	66.83	488.31	25174.1	
	04LongSST	single	30.16	10.13	53.06	635.75	18814.56	
		paired	33.28	9.94	73	498.52	26956.82	
	05NearSLR	single	29.64	10	59.43	529.42	21483.81	
		paired	31.63	9.88	71.67	467.16	27790.66	
	06LongSLR	single	29.66	10	58.23	536.5	20076.06	
		paired	32.89	10.07	72	490.57	25646.38	
	07NearCO2	single	32.25	10.88	54.34	642.27	19656.07	
		paired	38.12	11.41	76.25	538.09	27327.28	
	08LongCO2	single	29.63	9.97	50.26	656.27	16064.97	
		paired	31.91	9.62	65.83	514.54	22839.75	
	09NearPM25	single	29.36	9.85	56.34	544.9	20278.84	
		paired	36.47	11.13	70.42	549.87	27619.02	
	10LongPM25	single	28.95	9.75	52.26	623.06	17787.09	
		paired	32.16	9.84	63.67	561.29	22918.46	
Std. error mean	01NearT	single	0.72	0.17	2.51	30.23	1192.99	
		paired	2.67	0.6	9.11	53.42	3393.83	
	02LongT	single	0.83	0.16	2.6	34.24	1215.88	
		paired	4.08	1	9.41	61.25	4035.72	
	03NearSST	single	0.6	0.14	2.6	34.59	1080.85	
		paired	2.25	0.28	7.45	40.56	2977.65	
	04LongSST	single	0.87	0.19	2.91	44.05	1189.82	
		paired	3.64	0.65	9.77	51.89	4216.38	
	05NearSLR	single	0.64	0.16	2.72	25.55	1072.97	
		paired	1.87	0.75	6	37.04	2382.96	
	06LongSLR	single	0.66	0.16	2.7	22.14	1038.97	
		paired	3.14	0.87	7.37	50.32	2677.83	
	07NearCO2	single	1.03	0.31	3.34	31.45	1429.01	
		paired	3.94	0.67	9.58	49.92	3969.73	
	08LongCO2	single	0.66	0.12	2.54	43.24	938.7	
		paired	2.93	0.49	7.46	44.31	3107.72	
	09NearPM25	single	1.11	0.29	2.76	23.01	954.22	
		paired	2.65	0.63	6.73	42.15	3486.96	
	10LongPM25	single	0.81	0.21	2.53	51.74	1190.17	
		paired	1.66	0.21	6.56	56.18	2815.41	
Median	01NearT	single	29.18	9.87	60	454.16	22816.85	
		paired	27.96	8.99	65.5	408.06	26378.1	
	02LongT	single	29.06	9.85	54	536.45	19048.63	
		paired	25.75	8.49	66.5	403.91	26891.85	
	03NearSST	single	28.81	9.93	53	533.87	20015.09	
		paired	28.63	9.54	53.5	499.67	24475.15	
	04LongSST	single	29.28	9.97	50	580.53	18738.52	
		paired	27.66	9.94	67	438.09	23553.26	
	05NearSLR	single	29.04	9.85	57	522.46	20520.23	
		paired	30.87	9.16	74.5	458.61	26892.28	
	06LongSLR	single	28.54	9.96	56	516.82	19925.46	
		paired	27.45	9.32	71	441.25	25065.54	
	07NearCO2	single	31.28	10.35	50	604.08	18096.9	
		paired	35.7	11.44	59.5	499.68	23160.18	
	08LongCO2	single	29.27	10	49	618.23	16119.56	
		paired	29.89	9.61	61.5	480.47	22533.31	
	09NearPM25	single	28.56	9.82	53	547.81	18741.36	
		paired	34.78	10.52	70	538.77	24338.31	
	10LongPM25	single	28.3	9.77	53	564.06	17442.67	
		paired	30.67	9.84	66	544.2	24325.92	
Standard deviation	01NearT	single	4.24	1	14.87	178.84	7057.84	
		paired	9.24	2.08	31.57	185.06	11756.56	
	02LongT	single	4.91	0.93	15.38	202.59	7193.23	
		paired	14.14	3.46	32.58	212.17	13980.13	
	03NearSST	single	3.55	0.81	15.38	204.64	6394.38	
		paired	7.78	0.98	25.8	140.5	10314.88	
	04LongSST	single	5.16	1.09	17.21	260.58	7039.09	
		paired	12.61	2.25	33.83	179.76	14605.98	
	05NearSLR	single	3.77	0.95	16.1	151.14	6347.8	
		paired	6.49	2.6	20.78	128.3	8254.83	
	06LongSLR	single	3.89	0.96	15.99	130.97	6146.61	
		paired	10.87	3	25.52	174.3	9276.27	
	07NearCO2	single	6.09	1.83	19.75	186.05	8454.14	
		paired	13.65	2.33	33.19	172.93	13751.54	
	08LongCO2	single	3.93	0.69	15.01	255.79	5553.42	
		paired	10.14	1.7	25.85	153.5	10765.45	
	09NearPM25	single	6.54	1.69	16.34	136.11	5645.24	
		paired	9.19	2.17	23.3	146.02	12079.2	
	10LongPM25	single	4.79	1.24	14.98	306.07	7041.12	
		paired	5.75	0.72	22.73	194.62	9752.87	

164

S4 Table. Gaze metrics for maps, fully broken down.165
166
167
168

Following the analysis presented in previous tables, this table further breaks down the same five gaze metrics by both viewing conditions (single and paired) and individual map stimuli (10 in total). To conserve space, only means and SEMs are reported: For the single viewing condition, each cell data is derived from a sample size of $N_{\text{Single}} = 35$. For the paired viewing condition, each cell data is based on a sample size of $N_{\text{Paired}} = 12$.

AOI	Total fixation count (N = 47)		Total fixation duration in s (N = 47)	Relative dwell time in %	
	Top	64737	34806.87	80.87%	
Bottom	18591	8232.07	19.13%		
AOI	Condition	Fixation count (N _{Single} = 35, N _{Paired} = 12)	Total fixation duration in s (N _{Single} = 35, N _{Paired} = 12)	Relative dwell time in %	
Top	Single	43959	24997.11	80.15%	
Bottom	Single	13917	6191.21	19.85%	
Top	Paired	20778	9809.76	82.78%	
Bottom	Paired	4674	2040.85	17.22%	
AOI	Condition	Map	Fixation count (N _{Single} = 35, N _{Paired} = 12)	Total fixation duration in s (N _{Single} = 35, N _{Paired} = 12)	Relative dwell time in %
Top	Single	01NearT	4422	2218.32	72.82%
Top	Single	02LongT	4395	2443.90	79.07%
Top	Single	03NearSST	4341	2478.18	81.57%
Top	Single	04LongSST	4413	2689.43	84.93%
Top	Single	05NearSLR	4650	2396.03	76.98%
Top	Single	06LongSLR	4725	2517.04	80.83%
Top	Single	07NearCO2	4116	2628.77	77.62%
Top	Single	08LongCO2	4254	2679.58	86.14%
Top	Single	09NearPM25	4239	2337.68	75.84%
Top	Single	10LongPM25	4404	2608.18	85.81%
Bottom	Single	01NearT	1731	828.10	27.18%
Bottom	Single	02LongT	1323	647.00	20.93%
Bottom	Single	03NearSST	1353	560.10	18.43%
Bottom	Single	04LongSST	1158	477.34	15.07%
Bottom	Single	05NearSLR	1590	716.57	23.02%
Bottom	Single	06LongSLR	1389	596.84	19.17%
Bottom	Single	07NearCO2	1590	757.79	22.38%
Bottom	Single	08LongCO2	1023	431.32	13.86%
Bottom	Single	09NearPM25	1677	744.90	24.16%
Bottom	Single	10LongPM25	1083	431.27	14.19%
Top	Paired	01NearT	2172	895.93	82.18%
Top	Paired	02LongT	2166	984.31	85.25%
Top	Paired	03NearSST	1905	868.74	79.45%
Top	Paired	04LongSST	2328	1068.20	89.16%
Top	Paired	05NearSLR	2016	874.97	76.84%
Top	Paired	06LongSLR	2262	1047.46	88.47%
Top	Paired	07NearCO2	2313	1187.84	86.55%
Top	Paired	08LongCO2	1914	929.20	80.89%
Top	Paired	09NearPM25	1935	1034.78	78.82%
Top	Paired	10LongPM25	1767	918.33	79.33%
Bottom	Paired	01NearT	513	194.26	17.82%
Bottom	Paired	02LongT	453	170.27	14.75%
Bottom	Paired	03NearSST	501	224.72	20.55%
Bottom	Paired	04LongSST	300	129.85	10.84%
Bottom	Paired	05NearSLR	564	263.75	23.16%
Bottom	Paired	06LongSLR	330	136.51	11.53%
Bottom	Paired	07NearCO2	432	184.67	13.45%
Bottom	Paired	08LongCO2	456	219.57	19.11%
Bottom	Paired	09NearPM25	600	278.01	21.18%
Bottom	Paired	10LongPM25	525	239.25	20.67%

169

S5 Table. Gaze metrics for maps divided into two AOIs.

This table serves as a supplementary, proof-of-concept exploration of fixation count, fixation duration (in seconds), and relative dwell time (in percentage) between two AOIs. The stimulus was divided into two parts as two AOIs: the top part covering the world map, and the bottom part covering the scale and its accompanying brief explanatory text. For stimuli displayed on a screen size of 1920 × 1080 pixels, the division line was set at the 767th horizontal pixel, marking the boundary between the map and scale areas. The table is organised into three sections: (a) Overall cumulative: At the top, presenting data aggregated across all viewing conditions and maps, showing how fixation metrics are distributed irrespective of specific conditions. (b) Divided by viewing conditions: In the middle, data are split between single and paired viewing conditions, highlighting differences in gaze behaviour between these contexts. (c) Fully broken down: At the bottom, data are detailed for each map and viewing condition individually, offering a granular look at interaction patterns. Across all metrics, an approximate 80-20% relative dwell time split was consistently observed between the upper (map) and lower (scale) parts of the stimulus.

Descriptives

	Condition	Total fixation duration in s	Normalised fixation duration in percentage	Fixation count	Average fixation duration in ms	Scanpath length in px
N	single	70	70	70	70	70
	paired	24	24	24	24	24
Mean	single	56.97	0.50	154.87	380.51	24196.75
	paired	72.09	0.50	216.88	359.95	37468.70
Std. error mean	single	2.40	0.01	7.07	11.41	1205.88
	paired	5.30	0.02	20.27	18.68	3332.50
Median	single	56.78	0.50	153.50	357.63	21697.80
	paired	65.30	0.50	219.50	341.29	36599.86
Standard deviation	single	20.10	0.07	59.19	95.50	10089.12
	paired	25.97	0.08	99.29	91.53	16325.86
Minimum	single	15.34	0.36	70	216.00	10718.39
	paired	41.40	0.36	75	236.78	11845.43
Maximum	single	106.25	0.64	307	790.08	63731.17
	paired	118.51	0.64	434	578.53	71705.66

181 **S6 Table. Gaze metrics for paintings.**

182 This table presents descriptive statistics for five gaze metrics observed while viewing paintings: total fixation
 183 duration (in seconds and as a percentage of total viewing time), fixation count, average fixation duration (in
 184 milliseconds), and total proxy scanpath length in pixels. The metrics are reported with the following statistics for
 185 each: observation size (N), mean (M), standard deviation (SD), standard error of the mean (SEM), minimum (Min),
 186 and maximum (Max) values. The data ($N_{\text{PaintingStimulus}} = 2$) are segmented into single ($N_{\text{SingleSample}} = 35$) and paired
 187 ($N_{\text{PairedSample}} = 12$) viewing conditions, allowing for a direct comparison of these metrics under different social
 188 viewing contexts.

Kruskal-Wallis

	χ^2	df	p	ϵ^2
Total fixation duration in s	6.06	1	0.014	0.07
Normalised fixation duration in percentage	0.00	1	1.000	0.00
Fixation count	6.54	1	0.011	0.07
Average fixation duration in ms	1.37	1	0.242	0.01
Scanpath length in px	13.20	1	<.001	0.14

189 **S7 Table. Nonparametric ANOVA (Kruskal-Wallis test) for paintings, comparing single
190 and paired viewing conditions.**

191 This table details the results of a nonparametric ANOVA (Kruskal-Wallis test) used to analyse the differences in
192 gaze metrics between single and paired viewing conditions for paintings. Despite the exploratory nature of the
193 research and the relatively low sample sizes ($N = 35$ for single and $N = 12$ for paired), significant differences were
194 observed only in total fixation duration, and proxy scanpath length, but not in fixation count or average fixation
195 duration. The table provides a detailed breakdown of the test results for each metric, including the chi-squared (χ^2)
196 values, degrees of freedom (df), p-values, and effect sizes (ϵ^2). Note, although there is not a consensus on effect size
197 interpretation, $\epsilon^2 < .08$ may be assumed to be small, $\epsilon^2 < .26$ assumed to be medium, $\epsilon^2 \geq .26$ assumed to be
198 large.

Descriptives

	AOI	Condition	Total fixation duration in s	Fixation count	Scanpath length in px	Normalised fixation duration in percentage	Average fixation duration in ms
Mean	Francesca	paired	65.584	205.583	30868.837	0.460	344.332
		single	58.860	159.714	21671.617	0.511	377.368
	Klint	paired	78.597	228.167	44068.566	0.540	375.576
		single	55.072	150.029	26721.878	0.489	383.652
Std. error mean	Francesca	paired	6.165	25.222	3515.467	0.020	26.324
		single	3.693	10.344	1327.448	0.011	16.343
	Klint	paired	8.472	32.535	5115.004	0.020	26.877
		single	3.094	9.733	1940.344	0.011	16.159

199

S8 Table. Gaze metrics for paintings, fully broken down.200
201
202
203

Following the analysis presented in previous tables, this table further breaks down the same five gaze metrics by both viewing conditions (single and paired) and individual painting stimuli (2 in total). To conserve space, only means and SEMs are reported: For the single viewing condition, each cell data is derived from a sample size of $N_{\text{Single}} = 35$. For the paired viewing condition, each cell data is based on a sample size of $N_{\text{Paired}} = 12$.

Frequencies of Category

Category	Response	Counts
Cognitive-emotional impairment	Never	187
	Rarely	95
	Sometimes	51
	Often	15
	Almost always	4
Functional impairment	Never	141
	Rarely	50
	Sometimes	19
	Often	5
	Almost always	5
Personal experience of climate change	Never	23
	Rarely	32
	Sometimes	33
	Often	31
	Almost always	13
Behavioral engagement	Never	2
	Rarely	25
	Sometimes	62
	Often	79
	Almost always	96

204 **S9 Table. Survey descriptive statistics by CCAS subscales.**

205 This table displays the counts of responses on the Climate Change Anxiety Scale (CCAS), categorised using a 5-
 206 point Likert scale ranging from “never” to “almost always”. The data are broken down into four subscales:
 207 cognitive-emotional impairment, functional impairment, personal experience of climate change, and behavioural
 208 engagement. Each subscale includes a different number of survey items, which results in varying total counts per
 209 subscale. Note that the sample size for this analysis is $N_{\text{Sample}} = 44$.

Correlation Matrix

		Subscale 1	Subscale 2	Subscale 3	Subscale 4
Subscale 1	Spearman's rho	—			
	df	—			
	p-value	—			
	Kendall's Tau B	—			
	p-value	—			
Subscale 2	Spearman's rho	0.586	—		
	df	42	—		
	p-value	<.001	—		
	Kendall's Tau B	0.484	—		
	p-value	<.001	—		
Subscale 3	Spearman's rho	0.426	0.340	—	
	df	42	42	—	
	p-value	0.004	0.024	—	
	Kendall's Tau B	0.341	0.270	—	
	p-value	0.002	0.019	—	
Subscale 4	Spearman's rho	0.454	0.428	0.460	—
	df	42	42	42	—
	p-value	0.002	0.004	0.002	—
	Kendall's Tau B	0.355	0.330	0.352	—
	p-value	0.001	0.004	0.002	—

210 **S10 Table. Survey correlation statistics for CCAS subscales.**

211 This table presents the correlation statistics for the four subscales of the Climate Change Anxiety Scale (CCAS).
 212 Initially, responses on the 5-point Likert scale ranging from “never” to “almost always” were treated as ordinal
 213 data, with values from 0 to 4 assigned to each response. Subsequently, the sum of scores for each subscale was
 214 calculated. Correlations between the subscales were analysed using both Spearman’s rho and Kendall’s tau-b to
 215 assess the linear relationships. The table includes both correlation coefficients, significance levels (p-values), and
 216 degrees of freedom (df) for Spearman’s rho. These metrics provide insight into the cross-correlational dynamics
 217 among the subscales. The analysis, conducted with a relatively small sample size of $N_{\text{Sample}} = 44$ (irrespective of
 218 viewing conditions), consistently reveals positive linear relationships between the subscales, indicating a coherent
 219 pattern of responses across different dimensions of climate change anxiety.

Correlation Matrix

		TOTAL Dwell time	TOTAL Fixation count	AVERAGE Fixation duration	AVERAGE Scanpath length
TOTAL CCAS	Spearman's rho	0.053	-0.037	0.03	0.014
	df	42	42	42	42
	p-value	0.731	0.81	0.848	0.927
Kendall's Tau B		0.048	-0.012	0.02	0.007
	p-value	0.649	0.911	0.847	0.943

220 **SII Table. Correlations between gaze metrics and total CCAS score.**

221 This table extends the analysis from the previous correlation table by examining the relationship between the total
 222 Climate Change Anxiety Scale (CCAS) score (treating it again as ordinal data) and four gaze metrics (as continuous
 223 data). The total CCAS score was calculated for each participant based on the cumulative sum of their responses
 224 on the 5-point Likert scale, based on the high positive linear correlation between its four subscales. The gaze
 225 metrics reported here include total dwell time, total fixation count, average fixation duration, and average proxy
 226 scanpath length. Correlation coefficients (Spearman's rho and Kendall's tau-b) along with p-values and degrees of
 227 freedom (df) are presented to assess the statistical significance of these relationships. No significant correlation was
 228 found between the total CCAS score and any of the gaze metrics, indicating that there is no apparent relationship
 229 between these relatively raw gaze metrics and self-reported anxiety scores as measured by the CCAS. Note that
 230 $N_{\text{Sample}} = 44$.

231 **SI File. The Climate Change Anxiety Scale (CCAS).**

232 From: Clayton, S., & Karazsia, B. T. (2020). Development and validation of a measure of climate change
233 anxiety. *Journal of Environmental Psychology*, 69, 101434. <https://doi.org/10.1016/j.jenvp.2020.101434>
234 The Climate Change Anxiety Scale is a 22-item measure of the emotional response to climate change. The
235 measure has four sub-scales including cognitive and emotional impairment, functional impairment, personal
236 experience of climate change, and behavioral engagement. The scale has been validated in the U.S.
237

ITEMS:

238 Please rate how often the following statements are true of you.

Cognitive-emotional impairment (Subscale 1)

- 240 1. Thinking about climate change makes it difficult for me to concentrate.
- 241 2. Thinking about climate change makes it difficult for me to sleep.
- 242 3. I have nightmares about climate change.
- 243 4. I find myself crying because of climate change.
- 244 5. I think, "why can't I handle climate change better?"
- 245 6. I go away by myself and think about why I feel this way about climate change.
- 246 7. I write down my thoughts about climate change and analyze them.
- 247 8. I think, "why do I react to climate change this way?"

Functional impairment (Subscale 2)

- 249 9. My concerns about climate change make it hard for me to have fun with my family or friends.
- 250 10. I have problems balancing my concerns about sustainability with the needs of my family.
- 251 11. My concerns about climate change interfere with my ability to get work or school assignments done.
- 252 12. My concerns about climate change undermine my ability to work to my potential.
- 253 13. My friends say I think about climate change too much.

Personal experience of climate change (Subscale 3)

- 254 14. I have been directly affected by climate change.
- 255 15. I know someone who has been directly affected by climate change.
- 256 16. I have noticed a change in a place that is important to me due to climate change.

Behavioral engagement (Subscale 4)

- 257 17. I wish I behaved more sustainably.
- 258 18. I recycle.
- 259 19. I turn off lights.
- 260 20. I try to reduce my behaviors that contribute to climate change.
- 261 21. I feel guilty if I waste energy.
- 262 22. I believe I can do something to help address the problem of climate change.

Response Options:

- 263 Never - 1
264 Rarely - 2
265 Sometimes - 3
266 Often - 4
267 Almost always - 5